



# Spray Coating Experiments: Setups and Methodologies

The eBook cover features a large white number '13' on the left, followed by 'Thin Films III' and the title 'Spray Coating Experiments: Setups and Methodologies'. Below the text are two small images: one showing a 3D surface profile with a scale bar of 50µm, and another showing hands in blue gloves applying a spray coating onto a substrate. The bottom left corner has the 'EVIDENT OLYMPUS' logo, and the bottom right corner has the 'WILEY' logo.

**The latest eBook from  
Advanced Optical Metrology.  
Download for free.**

*Spray Coating Experiments: Setups and Methodologies*, is the third in our Thin Films eBook series. This publication provides an introduction to spray coating, three article digests from Wiley Online Library and the latest news about Evident's Image of the Year Award 2022.

Wiley in collaboration with Evident, are committed to bridging the gap between fundamental research and industrial applications in the field of optical metrology. We strive to do this by collecting and organizing existing information, making it more accessible and useful for researchers and practitioners alike.

EVIDENT™  
OLYMPUS

WILEY

# Recent Advances in Mechanical Vibration Energy Harvesters Based on Triboelectric Nanogenerators

Taili Du, Fangyang Dong, Ziyue Xi, Meixian Zhu, Yongjiu Zou,\* Peiting Sun,\* and Minyi Xu\*

**With the development of autonomous/smart technologies and the Internet of Things (IoT), tremendous wireless sensor nodes (WSNs) are of great importance to realize intelligent mechanical engineering, which is significant in the industrial and social fields. However, current power supply methods, cable and battery for instance, face challenges such as layout difficulties, high cost, short life, and environmental pollution. Meanwhile, vibration is ubiquitous in machinery, vehicles, structures, etc., but has been regarded as an unwanted by-product and wasted in most cases. Therefore, it is crucial to harvest mechanical vibration energy to achieve in situ power supply for these WSNs. As a recent energy conversion technology, triboelectric nanogenerator (TENG) is particularly good at harvesting such broadband, weak, and irregular mechanical energy, which provides a feasible scheme for the power supply of WSNs. In this review, recent achievements of mechanical vibration energy harvesting (VEH) related to mechanical engineering based on TENG are systematically reviewed from the perspective of contact–separation (C-S) and freestanding modes. Finally, existing challenges and forthcoming development orientation of the VEH based on TENG are discussed in depth, which will be conducive to the future development of intelligent mechanical engineering in the era of IoT.**

## 1. Introduction

With the development of autonomous/smart technologies, the IoT, artificial intelligence, big data, and the Fourth Industrial Revolution, intelligence has attracted more and more attention and become a promising development orientation in different fields.<sup>[1]</sup> Nowadays, a large number of machinery, vehicles, and structures related to mechanical engineering have been indispensable in human production and living. And intelligence

level of machinery, vehicles, and structures, which is related to mechanical engineering, plays a crucial role in industrial and social fields closely related to human life. It is of great importance to achieve comprehensive and continuous monitoring of them for improving their intelligent level. To achieve this, a great deal of distributed WSNs is extremely needed. Providing a sustainable power source for these WSNs has become the research focus. At present, the power supply method of plentiful sensors mainly includes cable and batteries in the industrial and social fields. On the one hand, powering through cable leads to high cost,<sup>[2]</sup> inconvenience, design and layout difficulties.<sup>[3]</sup> Moreover, damage to the cable resulting from vibration, high temperature, high humidity, and human causes,<sup>[4]</sup> will lead to low reliability and losing the monitoring function. On the other hand, powered by batteries faces with short life and periodic charging or replacement of the battery, which will lead to high maintenance cost and workload increase.<sup>[5]</sup> In addition, manufacturing and post-treatment of the battery will bring out environmental pollution because of its chemical properties.<sup>[6]</sup> Meanwhile, ambient energy, including solar,<sup>[7]</sup> wind,<sup>[8]</sup> and wave energy,<sup>[9]</sup> is widely distributed in the surrounding environment. These energies are treated as the macro renewable energy alternatives to traditional fossil fuel, not an option of the conventional battery for micropower supply. Furthermore, in the wake of increasing enhancement of design, manufacturing, and production, WSNs are becoming more miniaturization and lower energy consumption.<sup>[10]</sup> At present, the power consumption of multitudinous commercial wireless acceleration sensors, temperature sensors, and pressure sensors are as lower as a few microwatts ( $\mu\text{W}$ ) to tens of milliwatts (mW).<sup>[11]</sup> Concerning such micro energy, more and more research focuses on scavenging ubiquitous vibration,<sup>[12]</sup> acoustic,<sup>[13]</sup> human motion,<sup>[14]</sup> and thermoelectric<sup>[15]</sup> energy. Especially for the mechanical vibration,<sup>[16]</sup> although the power density of mechanical vibration is about  $10\text{--}300 \text{ mW cm}^{-3}$ ,<sup>[16b,17]</sup> it has some unique characteristics, including clean, deployment availability, minimal maintenance cost, and preserves the environment in an original state,<sup>[18]</sup> and is wide spreading in the industrial and social field. It can be an ideal candidate for powering plenty of

T. Du, F. Dong, Z. Xi, M. Zhu, Y. Zou, M. Xu

Dalian Key Lab of Marine Micro/Nano Energy and Self-Powered Systems

Marine Engineering College

Dalian Maritime University

Dalian 116026, China

E-mail: zouyj0421@dlnu.edu.cn; xuminyi@dlnu.edu.cn

T. Du, M. Zhu, Y. Zou, P. Sun

Collaborative Innovation Research Institute of Autonomous Ship

Dalian Maritime University

Dalian 116026, China

E-mail: sunptg@dlnu.edu.cn

 The ORCID identification number(s) for the author(s) of this article can be found under <https://doi.org/10.1002/smll.202300401>.

DOI: 10.1002/smll.202300401

distributed sensors, especially in indoor environment without solar and wind energy, such as ship engine room,<sup>[19]</sup> factory,<sup>[20]</sup> building interior.<sup>[21]</sup> Therefore, it will be of great significance to harvest vibration energy efficiently and achieve an in situ power supply for the WSNs in intelligent mechanical engineering.

At present, piezoelectric,<sup>[22]</sup> electromagnetic,<sup>[23]</sup> and electrostatic<sup>[24]</sup> are broadly applied to carry out VEH in the areas related to mechanical engineering. Scholars have launched a great many beneficial researches and achieved a series of outstanding outcomes on VEH based on the above technologies due to their own unique advantages.<sup>[16]</sup> However, piezoelectric vibration energy harvesting (PVEH), which is general cantilever structure, still faces problems such as narrow frequency band, piezoelectric material fatigue, and relatively low conversion efficiency.<sup>[25]</sup> Electromagnetic vibration energy harvester (EMVEH), which adopts Faraday's law, has some challenging in relatively complicated structure in microscales or nanoscales, low output voltage, and magnetic deterioration.<sup>[26]</sup> Even more, an electrostatic vibration energy harvester requires external voltage source.<sup>[24]</sup>

Since TENG was invented by Wang's group in 2012,<sup>[27]</sup> it aroused a large group of researchers' interests due to its high power density, diversity of material selection, easy to fabrication, versatile operation modes, environmental suitability, flexibility, robustness, and so on.<sup>[28]</sup> TENG is based on the combination of triboelectrification and electrostatic induction,<sup>[27]</sup> which is capable of converting different mechanical energies into electric power. Numerous remarkable works have been accomplished in various mechanical energy harvesting realizing sustainable power supply for abundant WSNs.<sup>[29]</sup> In addition, different self-powered sensors based on TENG have been developed in addition to be an energy harvester.<sup>[30]</sup> Moreover, many studies have been reported focusing on structure design,<sup>[31]</sup> theoretical analysis,<sup>[28,31]</sup> surface modification,<sup>[32]</sup> and material comparison<sup>[33]</sup> to improve the energy harvesting performance of TENGs. More than the above range of applications, TENGs are highly adaptable for VEH in the field related to mechanical engineering, in which the vibration frequency covers a broad band from less than 1 Hertz to hundreds of Hertz.<sup>[34]</sup>

A variety of researchers have presented plentiful innovative studies on VEH based on TENG over the past few years, which include vertical C-S mode, sliding mode, single-electrode mode, and freestanding mode. Recently, multitudinous outstanding review articles discussing VEH based on TENG have already been published,<sup>[11,31a,35]</sup> however, these studies involve quite a broad scope of the issues either including different types of energy in a certain field, or referring to diverse VEH methods. Over the years, vibration energy related to mechanical engineering is deemed to be the review article concentrating on VEH based on TENG in the fields of mechanical engineering is still vacant. The general vibration related to mechanical engineering is mainly excited by the working of the machinery itself or external forces impacted on structures such as wind, waves, and earthquakes, which usually represented by vibration frequency, amplitude, velocity, displacement, or acceleration.<sup>[36]</sup> Regarding adaptability to the working environment of mechanical engineering, the C-S mode and the freestanding mode (mainly C-S freestanding mode) are the two best choices in VEH based on TENG. The C-S mode is applicable to the

vertical C-S (VCS) movement in a cycle<sup>[37]</sup> and beneficial for energy harvesting.<sup>[38]</sup> As for the freestanding mode, because of the free layer, more mechanical motion types can be accepted.

**Figure 1** exhibits the specific architecture of this review, which aims to provide a comprehensive and systematic review of VEH based on TENG related to mechanical engineering from the aspects of C-S mode and freestanding mode for the first time. In the first part, the VEHs based on C-S mode TENG, including spring-based, analogous-spring, single cantilever, and multi-cantilever type, are discussed systematically. Subsequently, we elaborated on the VEHs based on freestanding mode TENG, which are divided into single-ball, multi-ball, flat, sliding surface, and deformable type. Finally, the challenge and future development orientation of the VEHs based on TENG related to mechanical engineering is summarized and prospected.

## 2. Working Mechanism of TENG

The theoretical foundation for TENG is based on Maxwell's displacement current (**Figure 2a**), which has been developed for more than a decade. Wang's group derived the expanded Maxwell's equations for a mechano-driven slow-moving media system recently:<sup>[57]</sup>

$$\nabla \cdot D' = \rho_f - \nabla \cdot P_s \quad (1)$$

$$\nabla \cdot B = 0 \quad (2)$$

$$\nabla \times (E - v \times B) = -\frac{\partial}{\partial t} B \quad (3)$$

$$\nabla \times [H + v \times (D' + P_s)] = J_f + \rho_f v + \frac{\partial}{\partial t} P_s + \frac{\partial}{\partial t} D' \quad (4)$$

where  $D'$  is the electric displacement field,  $\rho_f$  is the space charge density of free charges,  $P_s$  is a polarization term in the displacement vector,  $B$  is the magnetic field,  $E$  is electromagnetic field,  $v$  is the translation velocity,  $H$  is the magnetizing field, and  $J_f$  is the local free electric current density, which primarily expand the applications of TENG in various fields.<sup>[58]</sup>

The working mechanism of TENG is mainly explained according to the theory of triboelectric effect and electrostatic induction. To well explain the contact electrification and charge retention phenomena of two different materials, Xu<sup>[59]</sup> and Wang<sup>[60]</sup> proposed a general electron cloud/potential model (**Figure 2b**) based on the basic electron cloud interactions. Until the two materials contact, the surface state electrons cannot migrate due to the trapping effect of the potential well. When the two materials come into contact, their electron clouds overlap, causing electrons in the asymmetric double potential well enter another potential well to strike a balance. The external performance is the transfer of electrons from one material to another. When the two materials are separated, due to the potential barrier, most electrons will not be transferred, but are remained in the material. In this way, there will be the same amount of charges with opposite polarity on the surface of different materials, and the electric field will be formed.

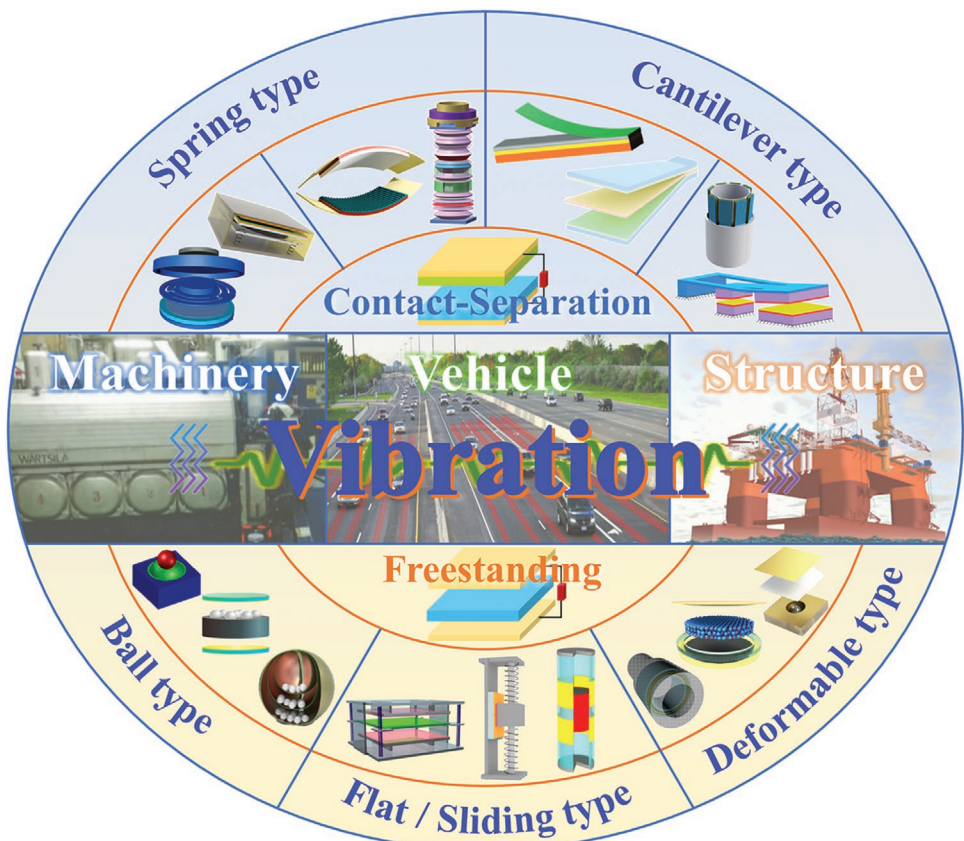


**Figure 1.** VEH based on TENG related to mechanical engineering. Adapted with permission.<sup>[39]</sup> Copyright 2022, Elsevier. Adapted with permission.<sup>[40]</sup> Copyright 2022, Elsevier. Adapted with permission.<sup>[41]</sup> Copyright 2022, Elsevier. Adapted with permission.<sup>[42]</sup> Copyright 2020, Elsevier. Adapted with permission.<sup>[43]</sup> Copyright 2018, Wiley-VCH. Adapted with permission.<sup>[44]</sup> Copyright 2022, American Chemical Society. Adapted under terms of the CC-BY license.<sup>[45]</sup> Copyright 2022, MDPI. Adapted under terms of the CC-BY license.<sup>[46]</sup> Copyright 2019, MDPI. Adapted with permission.<sup>[47]</sup> Copyright 2019, Wiley-VCH. Adapted with permission.<sup>[48]</sup> Copyright 2020, Elsevier. Adapted with permission.<sup>[49]</sup> Copyright 2022, Elsevier. Adapted under terms of the CC-BY license.<sup>[50]</sup> Copyright 2019, Elsevier. Adapted with permission.<sup>[51]</sup> Copyright 2014, American Chemical Society. Adapted with permission.<sup>[52]</sup> Copyright 2020, American Chemical Society. Adapted with permission.<sup>[53]</sup> Copyright 2016, Elsevier. Adapted with permission.<sup>[54]</sup> Copyright 2022, Wiley-VCH. Adapted with permission.<sup>[55]</sup> Copyright 2021, Elsevier. Adapted with permission.<sup>[56]</sup> Copyright 2017, American Chemical Society.

TENGs can be classified into four basic working modes according to the direction of polarization change and electrode arrangements, which are VCS, lateral sliding, single electrode, and freestanding layer modes. As mentioned above, C-S and freestanding layer mode, the typical models of which are shown in Figures 2c and 2d,<sup>[28]</sup> respectively, are more compatible with mechanical vibration. For the C-S mode, the two dielectric plates are stacked face to face as two triboelectric layers. At the outer surface of them, two metal layers are deposited as two electrodes. When two triboelectric layers with different material polarity come into contact with each other under the agitation mechanical force, their surfaces generate positive and negative charges as a result of the contact electricity. When the two triboelectric layers are separated, the positive and negative charges generated by electrical contact are also separated. The charges separation creates a potential difference between the top and bottom electrodes, which drives electrons through an external circuit between the two electrodes. When the contact state changes alternately, electrons flow into and out of the external circuit repeatedly, resulting in a continuous

alternating current (AC) output.<sup>[38]</sup> And for the freestanding mode, a dielectric plate and two metal plates are stacked face to face, forming two triboelectric pairs. The two metal plates also serve as two electrodes. After the dielectric plate being forced to contact with the two metal plates, both the top and bottom surfaces will have negative triboelectric charges due to contact electrification. The two metal plates will have the same amount of positive charges in total because of charge conservation. Similarly, the contact state of the dielectric plate and two electrodes causes electrons to transfer through the external circuit.

As mentioned above, on account of its produced conditions, most vibration energy related to mechanical engineering is represented by frequency, amplitude, velocity, displacement, and acceleration. Based on the working mechanism, the TENG can convert mechanical energy into electrical output signals, such as voltage, current, and charge. For VEH based on TENG, the vibration sources will be harvested and converted into electricity for powering sensor nodes and self-powered sensing system, as shown in Figure 2.

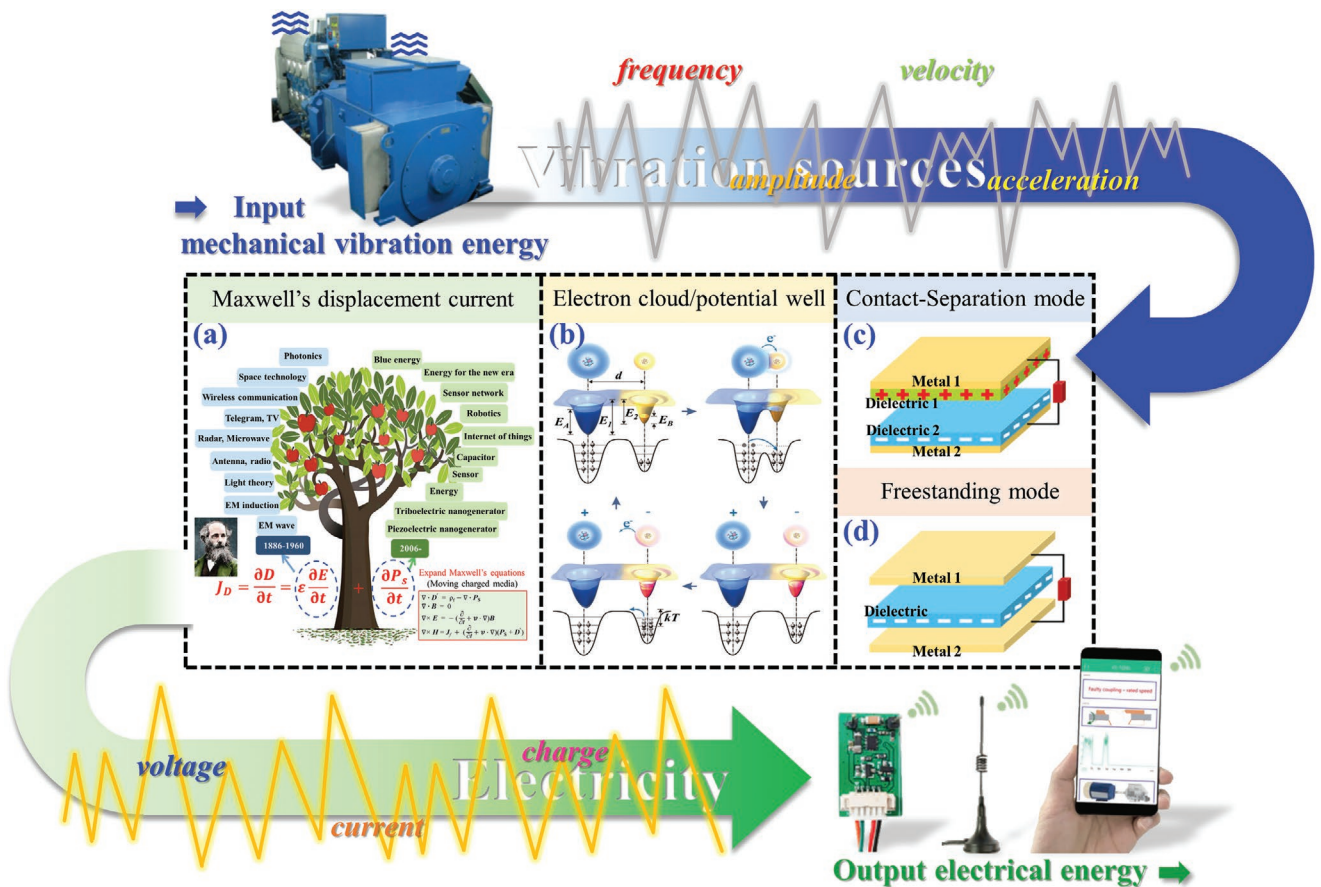


**Figure 2.** Workflow of mechanical vibration energy converting into electrical energy through TENG. Adapted with permission.<sup>[40]</sup> Copyright 2022, Elsevier. Adapted with permission.<sup>[61]</sup> Copyright 2022, Wiley-VCH. a) Theoretical foundation for TENG based on Maxwell's displacement current. Adapted with permission.<sup>[58]</sup> Copyright 2021, Elsevier. b) Electron cloud/potential well model for contact electrification. Adapted with permission.<sup>[59]</sup> Copyright 2018, Wiley-VCH. The TENG models for c) C-S mode and d) freestanding mode.

### 3. VEH Based on C-S Mode TENG

As energy conversion by VEHs based on TENG is accomplished by the tribo-electrification and electrostatic induction under the external excitation involving at least two different materials, C-S mode is the most straightforward design of the VEH based on TENG.<sup>[62]</sup> Most of the two different triboelectric materials are directly attached to two independent rigid insulating shell plates. Vibration directly acts on one of the shells, causing relative displacement with the other, leading to contact and separation of two face-to-face triboelectric surfaces. To separate the triboelectric layer persistently to ensure the continuity of power generation, researchers have introduced springs, analogous springs, and cantilever structures<sup>[35c]</sup> as essential frameworks between the two plates. To adopt the C-S mode TENG in VEH, well-design, vibration adaptability, and superior output power should be emphasized. Given these considerations, this section focuses on VEHs based on C-S mode TENG by distinct essential frameworks.

#### 3.1. Spring-Based VEH

Spring-based VEH is one of the earliest C-S mode TENGs applied to harvest mechanical vibration energy. It ensures

continuous contact and separation between triboelectric materials through the reciprocating movement of vibration-excited springs. With the assistance of the spring, vibration energy can be converted to electric power through C-S mode TENG triggered by continuous contact and separation between two tribo-materials resulting from mechanical vibration. As far back as 2013, Hu et al.<sup>[63]</sup> designed a suspended 3D spiral structure (single spring) TENG for VEH, which has a wide working bandwidth of 30 Hz, and the maximum output power density of 2.76 W m<sup>-2</sup> on a load of 6 MΩ. Toward higher power output, some upgraded structures based on a single spring were subsequently proposed.

Among them, Yuan et al.<sup>[39]</sup> proposed a metamaterial-inspired TENG (META-TENG) to harvest low-frequency mechanical vibration. As shown in Figure 3a, META-TENG consists of a proof mass, a protecting cap, a connector, a planar spring, Ecoflex/multi-walled carbon nanotubes (MWCNT) composite, a bottom part, and a spacer. Fluorinated ethylene propylene (FEP) film together with aluminum (Al) film, is attached to the lower side of the planar spring, and acts as one of tribo-materials and electrodes, respectively. The other Al film is below the Ecoflex/MWCNT composite to be the second electrode. The working principle of META-TENG is illustrated in Figure 3b. Here, the MWCNT doping and mixing with

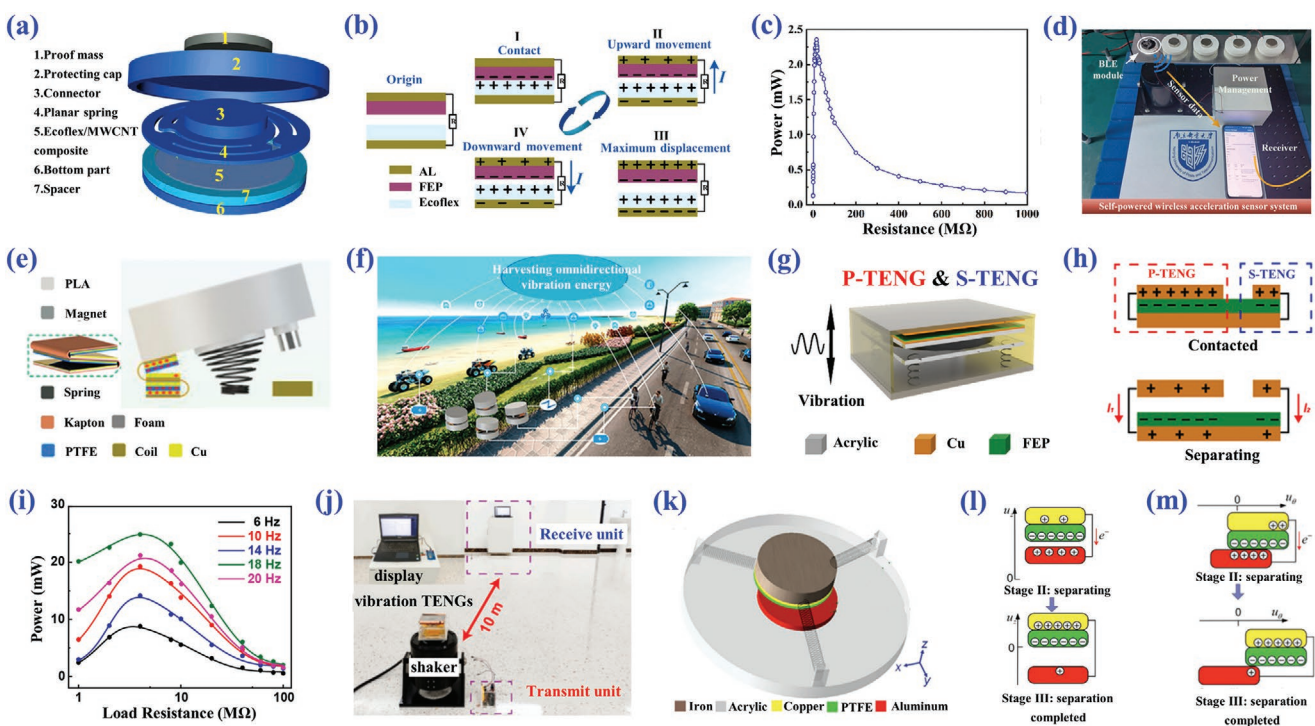


**Figure 3.** Spring-based VEH. a) Schematic diagram and b) working principle of the META-TENG. c) Power curve versus load resistance of the META-TENG for performance evaluation. d) Self-powered vibration monitoring. Reproduced with permission.<sup>[39]</sup> Copyright 2022, Elsevier. e) Structure diagram and f) application scenario of the OD-TENG. Reproduced with permission.<sup>[66]</sup> Copyright 2022, American Chemical Society. g) Schematic structure and h) working mechanism of the P-TENG and S-TENG. i) The power of the P-TENG with different load resistances at different frequencies. j) Demonstration of the P-TENG's power supply in a simulated vibration environment. Reproduced with permission.<sup>[40]</sup> Copyright 2022, Elsevier. k) Schematic of the 3D-TENG. l) Vertical C-S mode and m) in-plane sliding mode of 3D-TENG. Reproduced with permission.<sup>[67a]</sup> Copyright 2013, Wiley-VCH.

the Ecoflex solution has improved the output performance of META-TENG due to the higher dielectric constant and capacitance of the material. As displayed in Figure 3c, the maximum output power is 2.36 mW with an external load of 16 MΩ. With the array of META-TENGs, 640 LEDs and a calculator could be powered successfully. In addition, the META-TENGs array is capable of powering Bluetooth low energy module and then wirelessly transmitting the vibration acceleration of a structure to a mobile phone, which is depicted in Figure 3d. On the other hand, Wu et al.<sup>[64]</sup> proposed a spring-mass-based TENG, which is designed with an inside spring and an outsider helical structure to elevate the contact area, thus enhance the output performance.<sup>[65]</sup>

In addition to high output, omnidirectional mechanical VEH is another research interest in various fields relevant to mechanical engineering. To better adapt to multi-directional energy harvesting, based on a tower spring, Cao et al. proposed an omnidirectional triboelectric nanogenerator (OD-TENG), which can harvest vibration energy from the vehicle-mounted environment to power portable electronic devices and environmental sensors continuously.<sup>[66]</sup> The OD-TENG is projected as three zigzag double-layer units composed of two pairs of TENGs as demonstrated in Figure 3e. Each pair of TENG is composed of Kapton as a double-layer connection network, copper (Cu) as a positive friction material and electrode, and polytetrafluoroethylene (PTFE) as a negative electrode material. With the help of a tower spring, OD-TENG can respond

to external excitation in both vertical and horizontal directions. The maximum instantaneous power realized by the double-layer TENG unit is about 65 μW when the external resistance is 100 MΩ at a frequency of 6 Hz and an amplitude of 1.5 mm. Since the OD-TENG performs omnidirectional and broadband VEH effectively, as shown in Figure 3f, it has been proved that it has a promising prospect in mechanical vibration energy collection for various vehicles. It is worth mentioning that the researcher also specifies that the capacitor can be charged to higher voltage benefits from the high voltage characteristic of TENG. The works of Yang, He, and Kim et al. also enabled multi-directional energy harvesting.<sup>[67]</sup> However, to this goal, more auxiliary, unique structures and materials are often led-in, such as multiple springs, spherical shells, and flowable friction layers, rather than a tower spring in Cao's work. Except for a single real spring, a spiral structure patterned on a copper plate,<sup>[68]</sup> a flexible beam,<sup>[69]</sup> a cross leaf spring,<sup>[70]</sup> a pair of pre-tensioned springs,<sup>[71]</sup> or a hinged-hinged PZT bimorph<sup>[72]</sup> was acted as a spring to pick up vibration energy.

Furthermore, to improve the working stability of the C-S mode TENG, more springs-assisted VEHs based on C-S mode TENG are presented. Although two springs,<sup>[73]</sup> three springs,<sup>[74]</sup> and more springs<sup>[71,75]</sup> types have been proposed, the four springs-assisted TENG is the most classic form. To begin with, Chen et al.,<sup>[76]</sup> two acrylic plates as supporting substrates separated by four springs installed at the corners, produce a peak power density of 726.1 mW m<sup>-2</sup>. And the TENG

successfully powered about 20 LED bulbs by harvesting vibrational energy from the operating engine. Recently, as depicted in Figure 3g, the two-TENGs systems reported by Zhang's group had become a new research hotspot.<sup>[40]</sup> This two-TENGs system is divided into two vibrational TENGs in the left and right directions of two acrylic plates, four springs fixed on the four corners act as the essential framework to achieve contact and separation between copper electrode and FEP film stimulated by mechanical vibration. One of the TENGs is arranged to accomplish VEH, named powder-based TENG (P-TENG), and the other is used for vibration sensing (spherical TENG [S-TENG]), as shown in Figure 3h. Two TENGs have different functions but the same VCS mode working principle. The maximum output power of P-TENG is above 8.8 mW when the vibration frequency increases from 6 to 20 Hz, which is exhibited in Figure 3i. Furthermore, as shown in Figure 3j, P-TENG has realized the power supply for wireless sensing data transmission, which shows the extensive applications and promising prospects in the IoT, big data, and smart factory.

In other works, they also proposed the up-and-down distributed dual TENGs system<sup>[74,77]</sup> installed on mechanical equipment and used the energy from vibration of machines to monitor their working state. Researchers have carried out a large number of experimental research and theoretical analysis on the four springs-assisted TENG.<sup>[78]</sup> Even more, surface nano-structures have been verified as an effective method to improve output performance of TENG.<sup>[76]</sup> With the same purpose, a series of works focused on surface modification by micro/nano-structures have been raised.<sup>[76,78b,e,h–j]</sup>

On the other hand, more specialized designs have been presented to solve the related problems. Wu sealed the springs-assisted TENG in a separately designed downhole measuring subsection, which can sense the working condition of downhole tools in real-time by collecting vibration energy generated while drilling.<sup>[79]</sup> Li et al. made this contact-mode TENG waterproof to scavenge mechanical energy from vibrating ocean pipes.<sup>[78d]</sup> Xu et al. demonstrated an integrate-and-fire TENG (IF-TENG) inspired by mantis shrimp to harvest mechanical energy with ultralow vibration speeds by introducing an IF component.<sup>[78g]</sup> The maximum power density reaches  $0.14 \text{ W m}^{-2}$ , about 70 times larger than the TENG without the IF component. D. Bhatia et al. connected multiple resonant TENGs in tandem to work collectively with broadband frequency vibrations from different vibration sources like cars and air compressors.<sup>[78a,80]</sup> Many hybrid generators, electromagnetic–triboelectric<sup>[78e,j,79]</sup> and piezoelectric–triboelectric–electromagnetic,<sup>[78f]</sup> also carried this form of four-corner spring supports to harvest mechanical vibration energy. Not satisfied with one surface to one surface contact, upgrade structures with multiple contact surfaces such as multilayer structure,<sup>[75]</sup> pagoda shape,<sup>[34b]</sup> folding structure,<sup>[78k,l]</sup> and helical structure<sup>[81]</sup> were developed.

Except for the VCS mode, sliding C–S mode (SCS) TENGs have also been discussed by a lot of scholars. Cylindrical sliding TENGs equipped with one or two springs have been developed as a common model through several recent works.<sup>[73,82]</sup> Inspired by the outline of the bow, Tan et al. proposed a bow-type TENG to efficiently convert low-frequency vibration energy into electrical energy.<sup>[83]</sup> However, these works can only collect vibrations in one direction. Yang et al. combined the VCS mode and

the SCS mode and designed a hybridization mode 3D-TENG, which is displayed in Figure 3k for harvesting random vibration energy in different directions.<sup>[67a]</sup> In Figure 3k, the top core is suspended and sliding relative to the bottom by three springs with a  $120^\circ$  angle between each other. A PTFE layer with the copper back electrode as one contact surface is adhered to the bottom side of the top core. And an aluminum film with nanopores is used as the other electrode and contact surface. Both can proceed with either VCS or SCS, as shown in Figure 3l,m. The maximum power density of  $1.45$  and  $1.35 \text{ W m}^{-2}$  is achieved under in-plane or out-of-plane, respectively. Intuitively, about 30–40 LED bulbs can be lighted directly under the oscillating of a transmission line or the rotation movement of a wheel, which proves the ability of the 3D-TENG of energy harvesting to apply in grid transmission lines and various types of vehicles.

### 3.2. Analogous-Spring VEH

Some VEHs based on TENG may not use real springs, but they can still achieve the function of spring with their material elasticity and structure design, named as analogous-spring VEH. More importantly, the analogous-spring VEH structure often directly involves in generating electricity as the triboelectric layer of TENG rather than merely as an auxiliary mechanism. This unique design ensures that TENG will be pressed and released without other elastic support, and the area of the friction layer will significantly increase in the limited volume,<sup>[84]</sup> which will bring a significant improvement in electrical output.<sup>[48]</sup>

Imitating the spiral of spring, Yang et al. designed a retractable multilayer spring-like-electrode TENG (SL-TENG) as depicted in Figure 4a.<sup>[85]</sup> SL-TENG employs spring steel as not only the skeleton but also the triboelectric layer and electrode. Benefiting from this pattern, as shown in Figure 4b, it can be installed on the car brace and vibrate with the damping spring to efficiently collect and convert vibration energy in a small volume. Figure 4c shows the working principle of the SL-TENG, each piece of PTFE generates negative charges on the surface and equal positive charges are generated on the surface of the steel. All of them are well contacted and separated by the synchronicity of ideal analogous spring structure. The roughness of the steel surface is improved after sanding treatment, leading to increase of the surface charge density of triboelectric layers. The SL-TENG electric output performance is demonstrated in Figure 4d that only three layers can reach a maximum of  $306 \mu\text{W}$  at an external load of  $4 \text{ M}\Omega$  under the frequency of  $10 \text{ Hz}$  and amplitude of  $5 \text{ mm}$ . Due to its unique structural design and material selection, SL-TENG can act as a spring and is widely used in elastic and damping environments. He et al. presented a TENG based on these two parallel spiral structures to capture more mechanical vibration energy,<sup>[84]</sup> and the maximum output power reaches  $0.88 \text{ mW}$  with the great improvement compared to that with  $306 \mu\text{W}$  of the single spiral SL-TENG.<sup>[85]</sup> Du et al. proposed a bellows-type nano-generating spring to replace the traditional spring for VEH and vibration attenuation,<sup>[42]</sup> which is illustrated in Figure 4e. A copper layer and a triboelectric layer are bonded to each folded surface at a trough of the bellows tube. Nitrile rubber and silicone rubber,

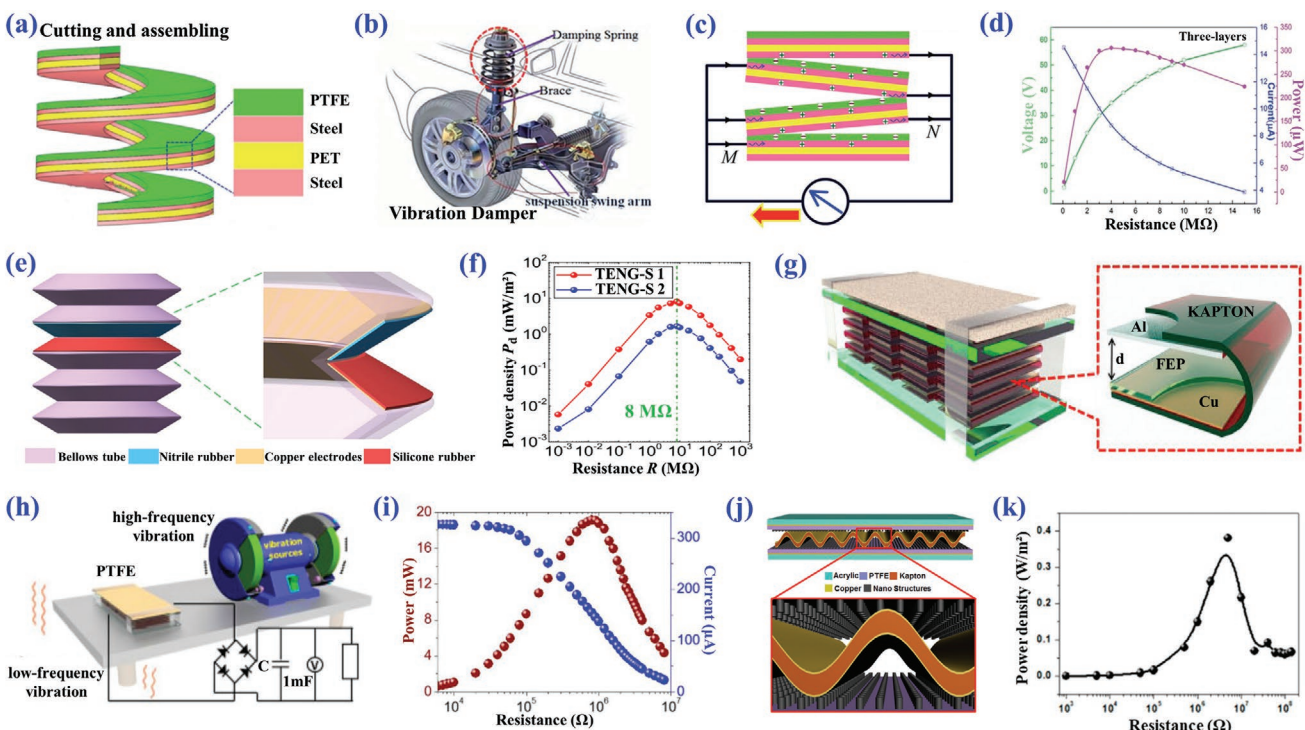


**Figure 4.** Analogous-spring VEH. a) Structure of the three-layer SL-TENG. b) Vibration damper of a car. c) Charge distribution and electricity generation process of the SL-TENG. d) Output voltage, current, and power versus different external resistances for the SL-TENG with three-layers, respectively (frequency of 10 Hz, amplitude of 5 mm). Reproduced under terms of the CC-BY license.<sup>[85]</sup> Copyright 2017, The Royal Society of Chemistry. e) Bellows-type triboelectric nanogenerator spring (TENG-S). f) Output power densities of TENG-S 1 and TENG-S 2 for different load resistances. Reproduced with permission.<sup>[42]</sup> Copyright 2020, Elsevier. g) Schematic diagram of the fabricated multiunit zigzag type TENG. h) System configuration of self-powered sensors for monitoring the running status of a running grinding machine. i) Dependence of the current and output peak power on the load. Reproduced with permission.<sup>[89]</sup> Copyright 2017, American Chemical Society. j) Schematic of the wavy-structured TENG. k) Output peak power density of the wavy-structured TENG dependent on the load resistance at the vibration frequency of 100 Hz. Reproduced with permission.<sup>[91a]</sup> Copyright 2014, American Chemical Society.

both of which achieve reciprocating C-S through extend and contract of the bellows tube. The output power density, as demonstrated in Figure 4f, performs  $15.72 \text{ mW m}^{-2}$  under a resonant frequency of 11 Hz and amplitude of 2 mm with a load resistance of  $8 \text{ M}\Omega$ . This energy transfer approach achieves both efficient vibrational energy collection of the TENG unit and structural vibration attenuation of the protected object. It opens up a new possibility for harvesting energy in systems that require vibration mitigation, such as landing gear of planes and cable dampers of the suspension bridge. Moreover, a cross-folded structure designed by Zheng<sup>[86]</sup> and an origami tessellation proposed structure by Zhang,<sup>[48]</sup> also became the highlights and achieved a wonderful collection effect. Both structures provide many layers of facets to install tribo-pairs and ensure that more contact tribo-surfaces participate in contact simultaneously within a motion cycle.

Besides the alike spring type, the arch is another typical structure of analogous-spring VEH, which can also conduct contact and rebound of two triboelectric layers with external excitation. For this purpose, the material used as an arch support tends to be flexible and has good elasticity. The surface treated single arch TENGs were pushed out one after another.<sup>[41]</sup> There is also a sandwich type TENG<sup>[87]</sup> with two arches and a clover type<sup>[88]</sup> with three arches. However, limited by the power generation, most of these arch-type analogous-spring TENG are generally

applied as sensors. Therefore, to promote the output performance, the stacking of layers is required. Wang et al. designed an elastic multilayered TENG unit to harvest low-frequency mechanical vibration energy.<sup>[89]</sup> As shown in Figure 4g, the multiunit TENG uses a zigzag-shaped Kapton film as the substrate to behave like a spring in response to external vibration. Al film and FEP film are designated as the triboelectric layers and attached to each zigzag Kapton structure, and the displacement between them will drive electrons flow in the external circuit. By combining a power management circuit (PMC), it can sustainably monitor the running statuses based on vibration energy harvested from a running grinding machine in Figure 4h. Furthermore, micropores and nanowires were prepared on the surfaces of Al and FEP films to enhance the charge density. Due to the larger contact area and micropores and nanowires prepared on the surfaces of Al and FEP films, it has high electrical outputs and low external resistance at such low frequency. Figure 4i shows that the maximum instantaneous power reaches  $19 \text{ mW}$  on the load of  $0.8 \text{ M}\Omega$  at 7 Hz. Additionally, by combining a PMC, it can sustainably monitor the running statuses based on vibration energy harvested from a running grinding machine, which demonstrates the potential applications in self-service equipment supervising, unmanned environment monitoring, and vehicular electronic power supply. Li et al. and Yang et al. proposed similar zigzag structures that had been successfully

applied to capture mechanical vibration energy from machine gears, bridges, and ships.<sup>[90]</sup> This multilayer structure possesses good integration ability and boosts output performance immensely.

In addition, some works directly take advantage of the elastic deformation of triboelectric layers to achieve contact and separation between each other.<sup>[91]</sup> Wen et al. invented a TENG with a wavy-structured Cu-Kapton-Cu sandwiched between two nanostructured PTFE films,<sup>[91a]</sup> which is displayed in Figure 4j. The special design allows self-restoration under mechanical vibration, rather than using extra springs or converting direct impact into lateral sliding, which is proved to be a more efficient contact mode for harvesting.<sup>[92]</sup> It is employed to harvest mechanical vibration energy from 5 to 500 Hz, and the peak power density reaches  $0.4 \text{ W m}^{-2}$  under a frequency of 100 Hz, as shown in Figure 4k. This scalable midbody maintains the sustainability of the TENG without spring, and can be easily packaged to apply for VEH. Besides, Zhao et al. developed a highly sensitive self-powered vibration TENG (VS-TENG) composed of foamed aluminum and FEP film with a gold-plated electrode.<sup>[61]</sup> Only with its elasticity, FEP film can repeatedly oscillate under the vibration excitation. Specifically, it has been resoundingly engaged in vibration detection for gearbox, compressors, etc., by converting the vibration to an electric signal, which may motivate its application in mechanical VEH.

### 3.3. Single-Cantilever VEH

In mechanical VEH, the cantilever beam is another classical configuration beyond the structure associated with the spring. On account of its advantages of simple structure, low-level input,<sup>[93]</sup> and large deformation,<sup>[94]</sup> the cantilever beam is widely put into practice in harvesting mechanical vibration energy. Among them, single-cantilever VEH based on TENG is a typical representative.<sup>[95]</sup> Chen et al. developed a kind of elastic-beam TENG (EB-TENG) with arc-stainless steel foil (arc-SSF),<sup>[43]</sup> which belongs to single-cantilever VEH. Figure 5a shows the schematic of EB-TENG. The arc-SSF, copper electrode, and PTFE film are pasted on the polymethyl methacrylate (PMMA) board. One end of the elasticity arc-SSF is fixed on the PTFE/Cu/PMMA structure, and the other part can touch the PTFE film under vibration excitation to achieve contact electrification. Working in C-S mode, the SSF and PTFE are positively and negatively charged, respectively. When they separate, based on electrostatic induction, the triboelectric charges are transferred between the SSF and the copper electrode through an external circuit. The peak value of open-circuit voltage generated by such a mini size, as depicted in Figure 5b, is  $\approx 28 \text{ V}$ , which indicates its potential for energy collecting.

To elevate the output performance of the single-cantilever VEH, two C-S pair mode TENG is presented. As shown in Figure 5c, Ren et al. proposed a trapezoidal cantilever-structure TENG (C-TENG) for wideband vibration energy extracting.<sup>[44]</sup> In this design, the aluminum coating is developed on two surfaces of FEP film as the positive triboelectric layer and the flexible vibration electrode, which is demonstrated in Figure 5d. With the flexible electrode sandwiched in two negative FEP layers, which forms a trapezoid, two TENG units are integrated

in one device. To enhance the surface charge density during contact electrification, the nanostructure on the surface of FEP film has been prepared by plasma etching. Because of these special settings, C-TENG can collect vibration frequencies from 1 to 22 Hz. The instantaneous output or power density is  $1.2 \text{ mW}$  or  $62.2 \text{ W m}^{-3}$  at 5 Hz, as illustrated in Figure 5e. Moreover, Figure 5f exhibits the visualized output performance of C-TENG, which is capable of lighting 120 LEDs under vibration frequency of 10 Hz. Furthermore, combining the array of six C-TENG units with a power management system, a self-powered wireless transmitting system is developed with success, which provides a practical strategy for self-powered application by harvesting mechanical vibration energy in a wide range from ultralow frequency (1 Hz) to high frequency.

Yang<sup>[96]</sup> and Quan<sup>[97]</sup> also designed sandwich cantilever beams to increase the contact area in small volumes. Unlike the usual design, Yang et al. added a mass to the middle cantilever beam based on the triple-cantilever TENG to improve the effectiveness of the cantilever beam,<sup>[96]</sup> which produces a peak power density of  $252.3 \text{ mW m}^{-2}$ . By direct use of the polydimethylsiloxane (PDMS) as the mass and a triboelectric layer to participate in C-S from the bottom part,<sup>[98]</sup> the peak power of the work proposed by the triboelectric layer achieves  $0.91 \mu\text{W}$  at 24.5 Hz. Even more, the tip mass can tune the resonant frequency of the cantilever beam in Zhao's work.<sup>[99]</sup> In addition, some other profiles related to the mass to improve the output performance of VEH have been invented.

Recently, a VEH consisting of a double-layered cantilever beam and a cambered shell was reported by Du et al.<sup>[100]</sup> and shown in Figure 5g. A magnet is fixed on the free end of the PET layer, which acts as a mass and takes part in electromagnetic power generation as well. The TENG is composed of a PTFE film coated with an aluminum electrode attached to the convex surface of polylactic acid (PLA) cambered shell and another aluminum coating as the electrode and triboelectric layer on the PET film. Employing the flexible PET film, when the cantilever beam vibrates, the aluminum electrode contacts and separates from the PTFE layer, and mechanical vibration energy is then converted into electricity. As shown in Figure 5h, the maximum power contributed by the TENG part is  $1.2 \text{ mW}$  at  $0.4 \text{ M}\Omega$  under 23 Hz. And then, the device succeeded in powering a multifunctional thermometer, as displayed in Figure 5i. For these designs, TENG increases the collectible frequency range and supplies a better charging performance.

What's more, different from the working mode of most cantilever-based VEH, Fu et al. developed a lateral sliding mode cantilever TENG,<sup>[101]</sup> as shown in Figure 5j, which composes of a beam clamped on a base and a slider attached to the other end. This VEH works in SCS mode with the slider sliding laterally on the bottom patches consisting of a triboelectric electrically active patch and a dielectric layer electrically inert patch without vertically separating (Figure 5k). Figure 5l shows the RMS voltage under different surface charge densities, and the RMS reaches almost 2 V under a frequency of 12 Hz and a charge density of  $200 \mu\text{C m}^{-2}$ . Although the lateral cantilever structure VEH with SCS mode is infrequent, it still provides a vital reference for designing new VEH configuration based on C-S mode TENG.

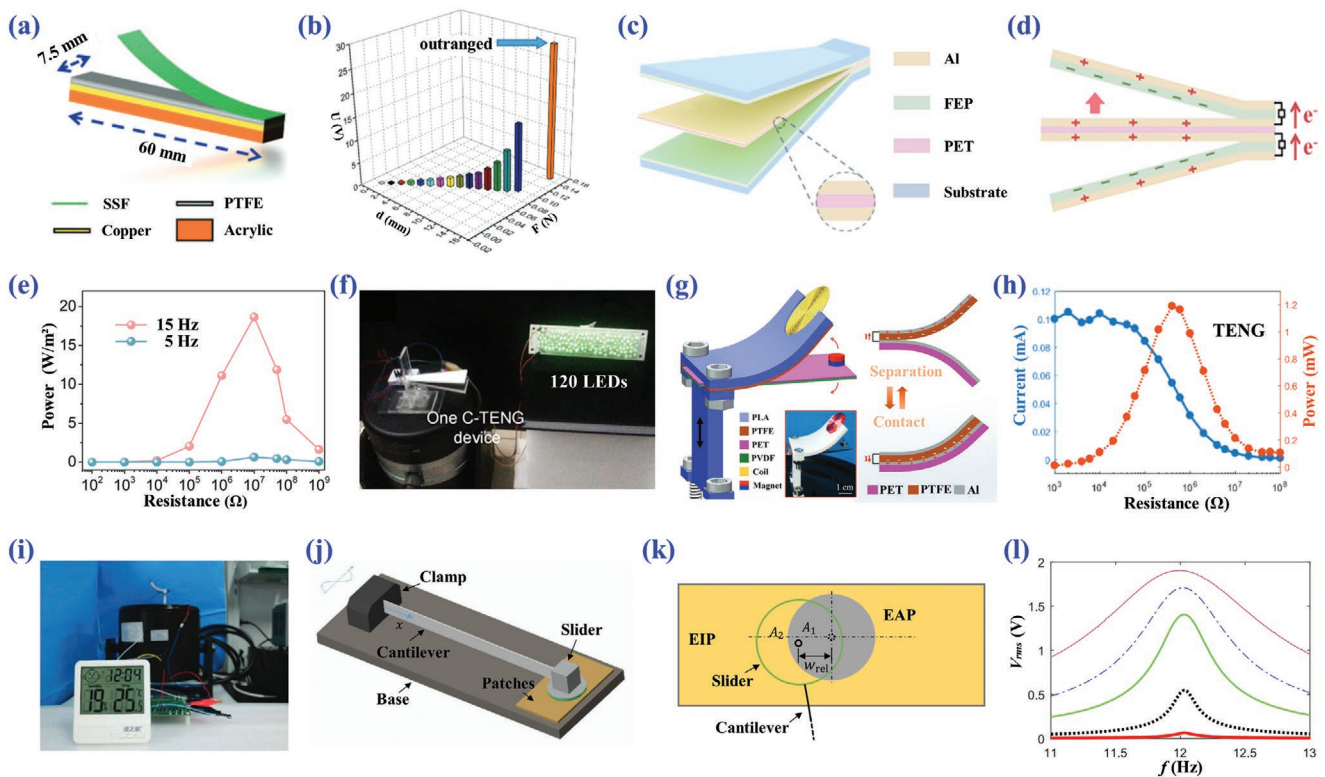


**Figure 5.** Single-cantilever VEH. a) Schematic of the EB-TENG. b) The experimental results of  $U$  versus  $d$  and  $F$ . Reproduced with permission.<sup>[43]</sup> Copyright 2018, Wiley-VCH. c) Structure and materials design of the C-TENG. d) Working principle of the C-TENG. e) Output power density of the C-TENG under different external loads. f) Photographs of the single C-TENG device powering the 120 LEDs at the vibration frequency of 10 Hz. Reproduced with permission.<sup>[44]</sup> Copyright 2022, American Chemical Society. g) Structure and working principle of the double layered cantilever beam TENG. h) Dependence of output current and output power of the double layered cantilever beam TENG on the external loading resistance. i) Demonstration of the power-supplying system sustainably driving a thermometer. Reproduced with permission.<sup>[100]</sup> Copyright 2018, Wiley-VCH. j) Configurations of the sliding mode cantilever TENG and k) the slider on patches. l) Frequency responses of the RMS voltage under different surface charge densities. Reproduced under terms of the CC-BY license.<sup>[101]</sup> Copyright 2020, IOP Publishing.

### 3.4. Multi-Cantilever VEH

Harvesting vibration energy in a wide bandwidth to the greatest extent is always one of the key objectives for TENG and other micro harvesters. On the basis of the characteristics of single-cantilever VEH based on TENG, cantilever beams with different lengths have different resonant frequencies.<sup>[102]</sup> On account of this, some piezoelectric nanogenerators have been presented.<sup>[103]</sup> Even more, as shown in Figure 6a, Han et al. produced a multi-cantilever VEH-based TENG, which integrates three cantilever beams with different lengths for broadband VEH.<sup>[104]</sup> Under mechanical vibration excitation, the bottom aluminum electrode will vibrate with the polyvinylidene fluoride (PVDF) cantilever beam leading to contact and separation with the PDMS layer, which is depicted in Figure 6b. The inverted pyramid microstructures with nanostructures are formed on the PDMS. It has to be mentioned that, during the electrification, the processed PDMS surface will greatly improve efficiency and output voltage of the TENG.<sup>[103b]</sup> At the first-order resonant frequency of 15 Hz, the generated peak-peak voltage is as high as 20 V, and a 1  $\mu$ F storage capacitor can be charged to 0.46 V in 120 s. Therefore, the TENG can effectively harvest vibration energy from the environment. And the output voltage under different frequencies is shown in Figure 6c, and three

peaks appear at 15, 32.5, and 47.5 Hz, respectively, which proves the effectiveness of wideband energy harvesting. The output performance of the device is greatly improved.

In addition to multiple individual cantilever beam, dividing a cantilever beam into the main beam and a secondary beam, Tang et al. proposed a two-degree-of-freedom (2DOF) cantilever vibration TENG to obtain higher operating bandwidth.<sup>[46]</sup> The structure of it is shown in Figure 6d, which consists of two TENGs with two top masses attached at the ends of the main and secondary beams and two corresponding bottom parts. The top part is composed of a glass substrate and an aluminum film that constitutes one triboelectric layer and the top electrode. In contrast, a PDMS film with microstructures is the other triboelectric layer and adheres to the bottom glass substrate with another aluminum film electrode. When the main beam and secondary beam start to vibrate, energy conversion is completed by C-S between aluminum and PDMS. The theoretical lumped-mass model of this TENG is established. The main and secondary TENGs have different peak power densities of 10.77 and 12.5  $\mu$ W cm<sup>-2</sup>, respectively, according to the test result, both of which are higher than many reported cantilever-based TENGs.<sup>[96,97,98b]</sup> Then, as exhibited in Figure 6e, this TENG was successfully applied on a vacuum compression pump for 5 h, showing its feasibility of powering in daily life,

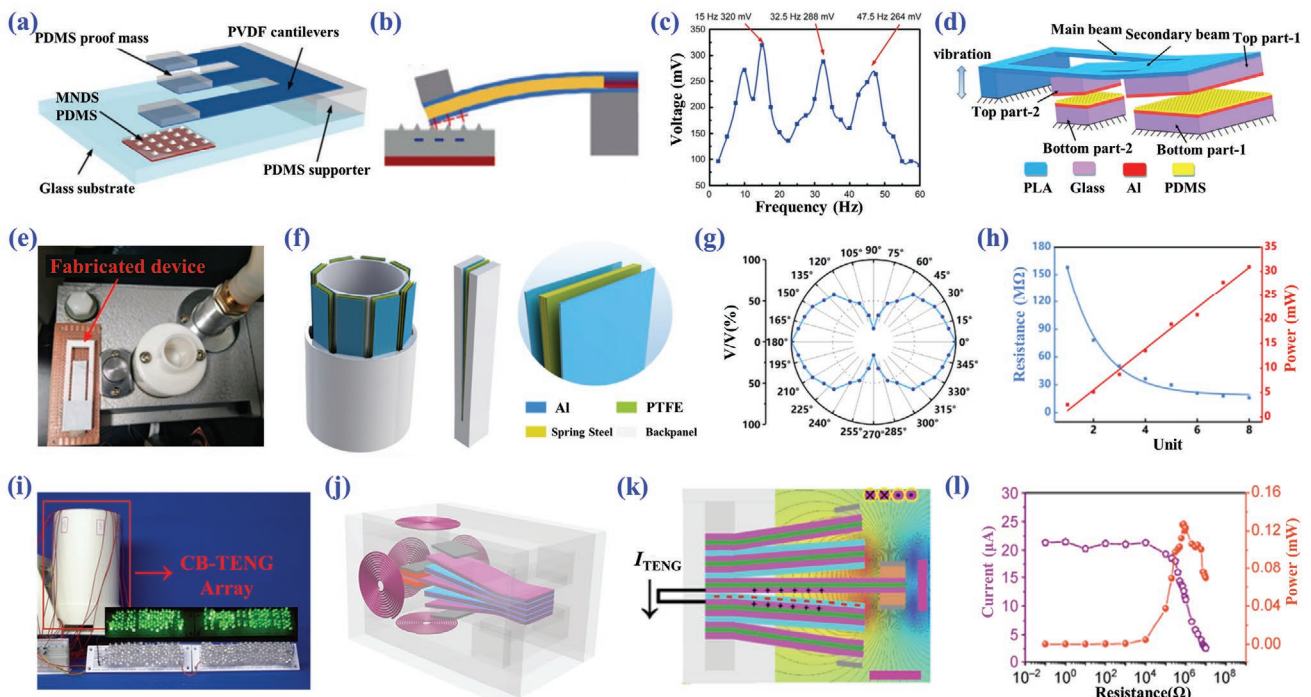


**Figure 6.** Multi-cantilever VEH. a) 3D view and b) working principle of the PVDF multi-cantilever VEH-based TENG. c) Output voltage of the PVDF cantilever array under different frequencies. Reproduced with permission.<sup>[104]</sup> Copyright 2013, Springer Nature. d) Schematic of the 2DOF cantilever vibration TENG. e) Application of the 2DOF cantilever vibration TENG on a vacuum compression pump. Reproduced under terms of the CC-BY license.<sup>[46]</sup> Copyright 2019, MDPI. f) The structure of array-type CB-TENG. g) The percentage of open-circuit voltage varies with azimuth. h) Dependence of the current and output power density on the external load resistance for the CB-TENG. i) Array-type CB-TENG lighting 204 LEDs. Reproduced under terms of the CC-BY license.<sup>[45]</sup> Copyright 2022, MDPI. j) 3D schematic diagram and k) working principle of the multilayer sandwich type TENG. l) Measured output currents and corresponding output powers of the multilayer sandwich type TENG. Reproduced with permission.<sup>[97]</sup> Copyright 2016, Springer Nature.

although with slightly decreasing in the 1st h. Moreover, Hu et al. designed a VEH with two TENG units fixed at two ends of a rod to harvest the vibration energy of transmission lines as well as vibration attenuation.<sup>[105]</sup> The response frequency range can be expanded five times by adding a movable mass roller, which boosts the bandwidth significantly. And the peak voltage, peak current, and peak power of the parallel TENG achieve 1002 V, 1775 μA, and 4.31 mW separately.

To further enhance the electrical output, an array-type vibration energy harvester integrated with eight cantilever-beam-based TENGs (CB-TENG) is designed by Lian et al. for transverse VEH of drill pipes,<sup>[45]</sup> which is illustrated in Figure 6f. In each unit, two vibrators structure like C-TENG<sup>[44]</sup> are set in CB-TENG, whose output voltage is 2.9 times than the one vibrator structure. To further utilize the internal space of the drill pipe and improve the electrical output, eight CB-TENGs are integrated along the circumference to form the array. Thanks to this unique design, CB-TENG can harvest vibration energy in the arbitrary transverse direction, and the voltage varying with azimuth is displayed in Figure 6g. In Figure 6h, the maximum peak power of the eight CB-TENGs in parallel has increased to 30.95 mW at a vibration frequency of 3 Hz. And 204 LED bulbs were successfully lit up, which is depicted in Figure 6i. A 30-day durability test was also performed, and the current output was only reduced by 2%, showing well robustness of it.

Instead of direct integration of single-cantilever VEHs based on TENG, Quan proposed a multilayer sandwich

type TENG through structural design to increase output in a novel way,<sup>[97]</sup> which is shown in Figure 6j. Figure 6k indicates that it consists of four TENGs based on five cantilever beams, both surfaces of each cantilever beam are plated with copper films. FEP films are attached on the surfaces of the second and fourth beams from the top down to be used as triboelectric materials. The vibration of the middle cantilever motivates copper and FEP films on each beam to periodically contact and separate, resulting in a current flow. Figure 6l shows the highest output power reaches about 0.13 mW under a load resistance of 0.8 MΩ. By integrating EMG in series, the TENG can charge a self-made Li-ion battery from 1 to 1.9 V in 6.3 h. Compared with the single-cantilever VEH in vibrational energy scavenging, the integration of multiple cantilevers brings wider bandwidth and larger triboelectric generating area to obtain a larger collection range and higher electrical output, which is one of the development trends of this structure.

In summary, different types of VEHs have been designed according to mechanical vibration characteristics and different working environments. A major objective of VEHs based on TENG is to improve power output performance; researchers have made a lot of progress in improving output performance by selecting different tribo-materials, increasing contact area through structural design, surface treatment, etc. For the VEHs based on C-S mode TENG, the use of spring, analogous-spring, and cantilever beam, concluded as elastic structure,

in C-S mode VEH not only guarantees the essential space between tribo-materials, which is crucial to the power generation of TENG, but also magnifies the amplitude of motion. So that, the C-S mode VEH can be excited by mechanical vibration of lower frequencies and lower amplitudes. Therefore, the C-S mode has been broadly applied in mechanical VEH in intelligent mechanical engineering. Furthermore, multilayer VEH based on C-S mode TENG has significantly improved due to its unique stack design and elastic structure. The VEHs based on C-S mode TENG primarily depend on the elasticity modulus of the elastic structure, which presents resonance characteristics. Therefore, most of the VEHs based on C-S mode TENG, regardless of spring, spring-like, or cantilever beam construction, present unique merits in VEH for machinery, vehicles, and structures working at relatively constant frequencies. Consequently, the prime output could be obtained if the resonant frequency of the VEH is in accordance with the vibration of machinery or structure. However, the durability of VEHs based on C-S mode TENG may be affected by the working life of springs and cantilever beams due to long-term operation. Although the elastic material of the analogous-spring structure has stronger toughness and longer service life, the resonant frequency of the elastic structure including the spring, cantilever beam, and analogous-spring is not easily adjustable, which also limits its application in wide frequency. Meanwhile, wideband frequency adaptability should be highlighted because of various working condition of the mechanical engineering. Therefore, it will need further research orientation to address favorable output under a relatively wide mechanical vibration frequency range by wideband frequency VEH design, including tunable elasticity of the elastic structure, and nonlinear VEH technology.

#### 4. VEH Based on Freestanding Mode TENG

Besides the VEH based on C-S mode TENG, because the nonlinear factors in the freestanding layer's stiffness allow the TENG to be efficient at collecting mechanical energy over an extensive frequency range,<sup>[106]</sup> VEHs based on freestanding mode TENG motive rapid progress in mechanical VEH based on TENG technology. Different from the C-S mode, the spring or analogous spring is not indispensable in the VEH based on freestanding mode TENG. Generally, there is no physical connection between the freestanding layer and the other triboelectric materials or electrodes. Under adequate external mechanical vibration, the freestanding layer will move or bounce between two limiters, leading to charge transfer between two electrodes, commonly installed on the limiters. In other aspects, VEH based on sliding freestanding mode TENG can also be utilized to harvest mechanical vibration energy with the assistance of some other structures. In any case, the freestanding layer is one of the critical factors, which will influence the output performance, as well as the mechanical VEH efficiency, to a great degree. Therefore, according to different freestanding layers, such as the single-ball type, multi-ball type, flat type, sliding surface type, and deformable type, the VEHs based on freestanding mode TENG are systematically discussed in this section.

##### 4.1. Single-Ball VEH

Single-ball VEH is one of the simplest configurations in VEHs based on freestanding mode TENG. The ball, as the free-standing layer in most cases, bounces or rolls on other tribo-materials or electrodes under external vibration, which will result in energy conversion because of the contact and separation between the ball and other parts. Among numerous studies, the bouncing ball system has raised much concern in the engineering due to its simplicity and the abundant dynamic behaviors in vibration systems.<sup>[107]</sup> To begin with, Du et al. proposed a bouncing-ball TENG (BB-TENG) to convert ship machinery vibration energy into electricity.<sup>[34a]</sup> As shown in Figure 7a, the BB-TENG consists of two copper electrode layers attached to two acrylic panels and PTFE ball inside the PLA container. Demonstrated through a high-speed camera, described in Figure 7b, the PTFE ball will bounce between the two electrodes driven by enough external vibrations. When the PTFE ball contacts the copper electrodes, due to different triboelectric polarities, the copper electrodes are positively charged, while the PTFE ball is negatively charged. Based on these, the continuous motion of the PTFE ball in the PLA container will generate continuous electric energy. As demonstrated in Figure 7c, the maximum power density is about  $3 \text{ W m}^{-3}$  with seven separate single-ball VEH integrated under a vibration frequency of 35 Hz, which can light up 30 LEDs, showing great potential to be a distributed power source. Additionally, the BB-TENG is practically arranged on an air compressor (shown in Figure 7d) to monitor the vibration condition. Guo et al. also take advantage of the PTFE ball's contact with the copper panel electrode, and achieve monitoring of equipment operation in real-time by converting vibration energy to electricity.<sup>[108]</sup> Moreover, Wang et al. proposed another self-powered multifunctional motion triboelectric sensor with polyurethane (PU) ball, PTFE film, and electrodes.<sup>[109]</sup>

To scavenge vibration energy in full space,<sup>[110]</sup> researchers designed a spherical space with metal electrodes adhered to its inner surface, which not only allows the ball to move  $360^\circ$ , but also increases the contact area between the ball and electrodes. Zhu et al. proposed a square-shell spherical cavity structure with the ball arranged inside,<sup>[49]</sup> as shown in Figure 7e, which is called PC-TENG consisting of PLA, silicone rubber ball, and copper electrode. Figure 7f shows that each half of the cavity is deposited with the copper electrode, and the silicon rubber ball will approach or principle the top and bottom electrodes under mechanical vibration. To improve the collection ability, they embedded five by five PC-TENG units in a plate-type structure for harvesting vibration energy from buildings and transportation systems, as shown in Figure 7g. According to the test results, the PC-TENG can efficiently collect mechanical energy as well as work as a vibration and shock absorber for some major buildings and equipment.

On the basis of the promotion in the electrode structure, more directly with a bigger ball over a small ball, as illustrated in Figure 7h, Wu et al. proposed a S-TENG to collect the down-hole vibration energy.<sup>[111]</sup> The composition of S-TENG is shown in Figure 7i. Here, a fixed ball shell is directly used to form a space for the free movement of the freestanding ball. The triboelectric materials are copper and PTFE, with the copper film

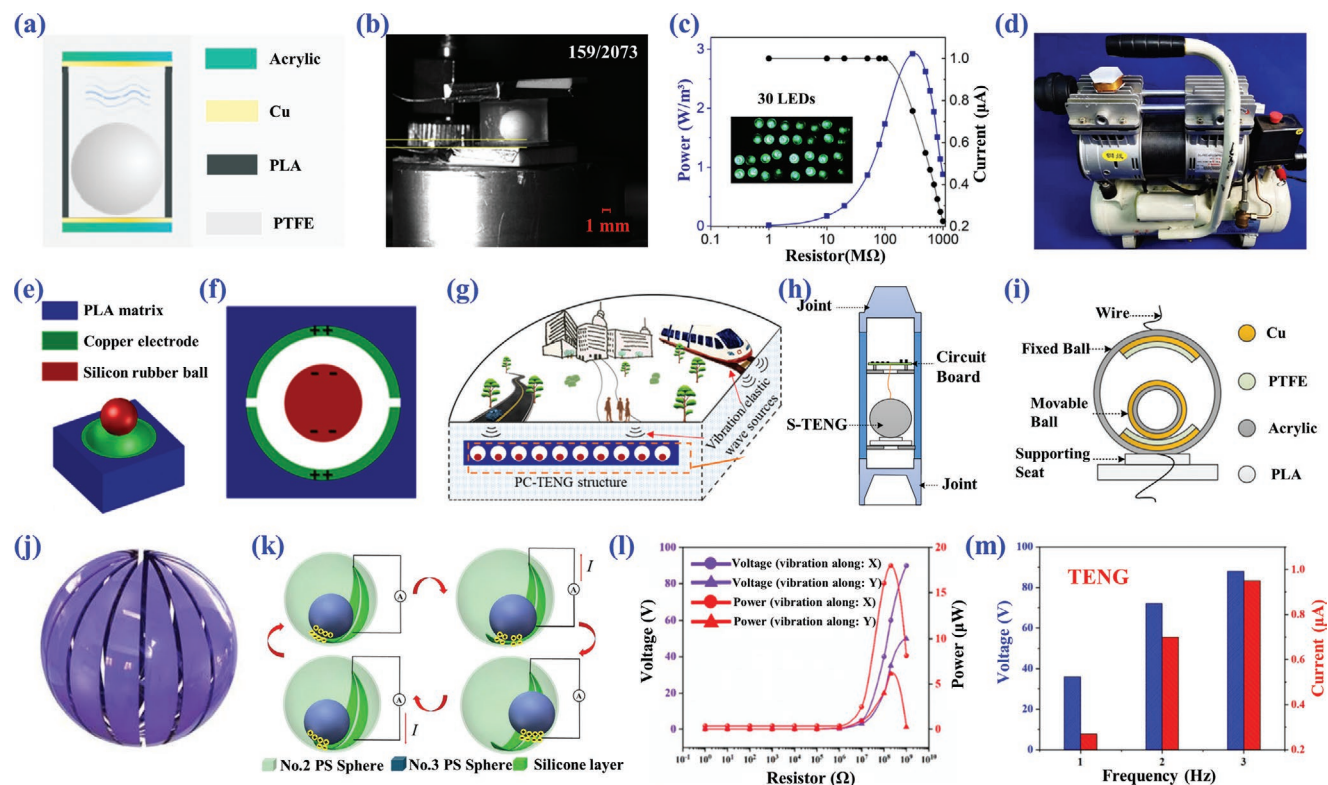


**Figure 7.** Single-ball VEH. a) Structure of the BB-TENG. b) PTFE ball-bouncing status demonstrated by using high-speed camera at the frequency of 25 Hz. c) Output power and current of the BB-TENG in series with different load resistors. d) The BB-TENG is arranged on the air compressor. Reproduced under terms of the CC-BY license.<sup>[34a]</sup> Copyright 2021, MDPI. e) Structure and f) working principle of the PC-TENG. g) PC-TENGs are used in the fields of some smart buildings or transportation systems. Reproduced with permission.<sup>[49]</sup> Copyright 2022, Elsevier. h) The downhole measuring instrument with the S-TENG. i) The downhole measuring instrument with the S-TENG. Reproduced under terms of the CC-BY license.<sup>[111]</sup> Copyright 2020, MDPI. j) Schematic diagram of the "Willow" friction layers. k) Charge generation process in TENG module. l) Voltage and power relationship diagram of the TENG with different excitation directions. m) Output performance of the TENG with different frequency. Reproduced with permission.<sup>[67b]</sup> Copyright 2020, Elsevier.

also serving as the electrode. The output power of S-TENG reaches the maximum value of  $10.9 \times 10^{-9}$  W. According to the test result, if the power generation is stored for a while with multiple S-TENGs connected in parallel, it is possible to provide intermittent power supply for low-power downhole measuring instruments. And similar to the S-TENG, Zhang et al. designed a spherical 3D-TENG, consisting of an outer spherical shell and an inner polyfluoroalkoxy ball, which can effectively scavenge vibration energy in full space as well.<sup>[110]</sup>

To further enhance the output performance, as shown in Figure 7j, He et al. presented six willow shape electrodes evenly to the inner surface of the spherical shell to transform 3D full-space mechanical energy.<sup>[67b]</sup> Instead of working in vertical contact, the internal plastic ball tends to roll back and forth between two pieces of copper electrodes in response to the vibration, as displayed in Figure 7k. It is worth mentioning that the plastic ball directly contacts with the silicone layer covered on six copper electrodes, which is possible to improve the sustainability of it. According to the triboelectric series, the plastic ball is more active than silicone rubber. Therefore, the plastic ball has positive charges, and the silicone layer preserves negative charges during the mechanical VEH process. Furthermore, the inverted pyramid structures are prepared on the surface of the silicone layer for the improvement of contact area and

triboelectric effect and then the output performance. As seen from Figure 7l, the maximum output power of TENG under the vibration in the x-axis or y-axis is 18 or 6 μW at an external resistance of 200 MΩ. And in Figure 7m, the voltage and current of the TENG in this work achieve 88 V and 0.95 μA under a vibration frequency of 3 Hz. Similar to the six electrodes in this work, a multi-electrodes array structure can greatly improve the space utilization rate and effectively increase the output power density,<sup>[112]</sup> for example, radial-arrayed rotary electrodes,<sup>[112b,113]</sup> fine-grating electrodes,<sup>[114]</sup> and interdigitated electrodes.<sup>[115]</sup>

#### 4.2. Multi-Ball VEH

On basis of single-ball VEH, using more balls as the free-standing layer to participate in charge transfer is a direct and effective method to improve the electrical output of TENG.<sup>[116]</sup> Some works put a number of electronegative balls between two parallel metal plates to harvest the vibrational energy.<sup>[117]</sup> First, Xiao et al. designed a honeycomb structure-inspired TENG (HSI-TENG),<sup>[47]</sup> as shown in Figure 8a, PTFE balls are filled in honeycomb grooves and vibrate in their own fixed orbits rather than moving in disarray. The effective contact area and the power density of the honeycomb structure are enhanced

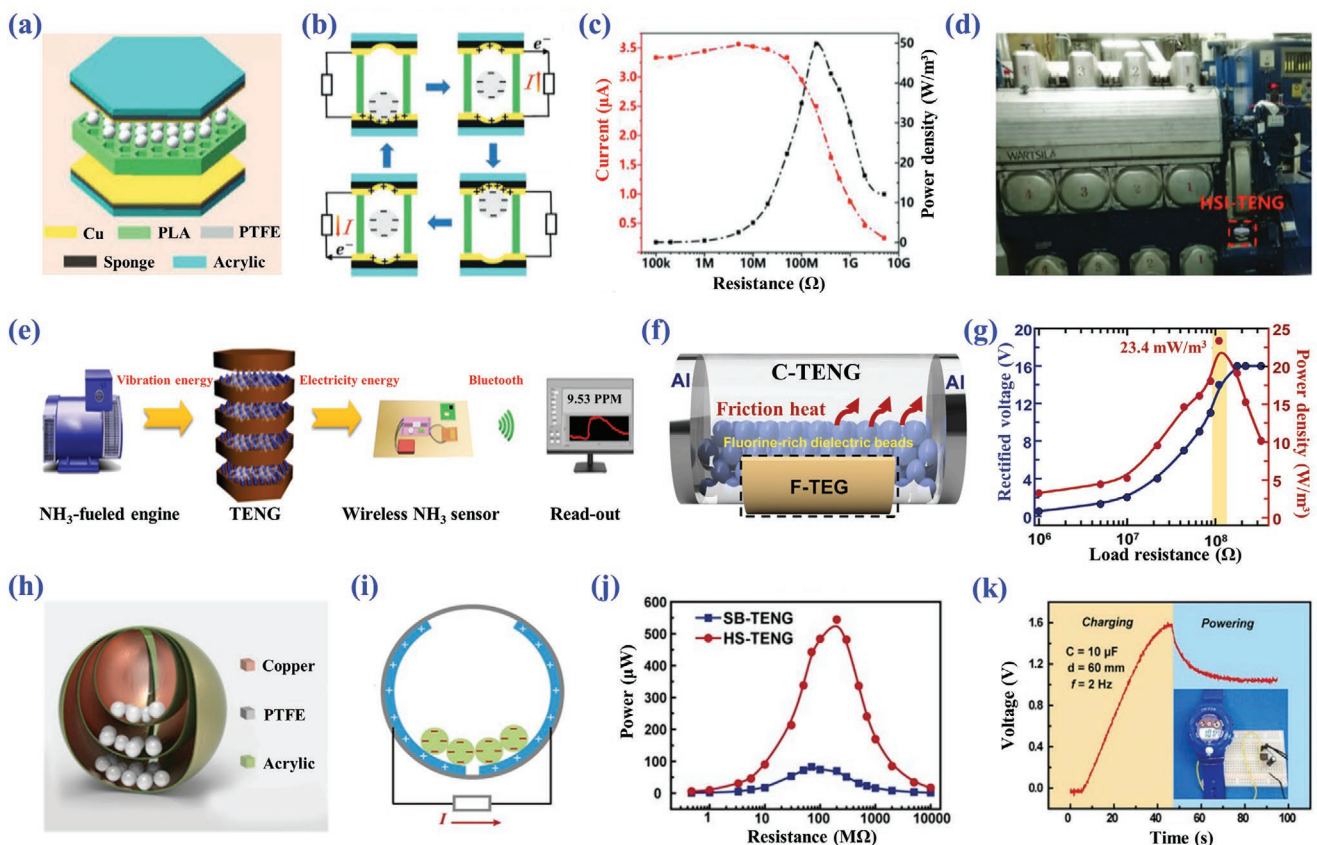


**Figure 8.** Multi-ball VEH. a) Structure and b) working mechanisms of the HSI-TENG. c) Dependence of the voltage and output power on the external load resistance for the HSI-TENG working at vibration frequency of 25 Hz and vibration amplitude of 2.0 mm. d) Photograph of HSI-TENG as a self-powered monitor for the diesel engine on the ship YuKun. Reproduced with permission.<sup>[47]</sup> Copyright 2019, Wiley-VCH. e) Schematic diagram of the self-powered full-set ammonia operation process. Reproduced with permission.<sup>[118]</sup> Copyright 2022, Elsevier. f) Schematic illustration of the hybridized generator to simultaneously harvest tribo-thermal energy induced by the vibration of the PTFE beads. g) Electrical output power density of the C-TENG acquired with the various load resistances. Reproduced with permission.<sup>[117c]</sup> Copyright 2022, Elsevier. h) Schematic structure of the HS-TENG by nesting three-layer spherical shells. i) Working principle of the HS-TENG. j) The comparison for the output powers of an HS-TENG and an SB-TENG at 2 Hz. k) Charging curve of the capacitor (10  $\mu$ F) while an electronic watch is driven by the HS-TENG. Reproduced with permission.<sup>[50]</sup> Copyright 2019, Elsevier.

by 12.2% and 43.2%, respectively, compared to that of square structure. Even more, the sponge is attached to the upper and lower electrodes to increase the contact area between the ball and the electrode. All these arrangements undoubtedly promote output performance. The HSI-TENG can generate electricity once the balls separate from the electrode, the theoretical mode of it is established, and the test results show that it is adaptable to harvest mechanical vibration energy from 10 to 60 Hz effectively. The PTFE ball in each groove forms a small TENG with its upper and lower electrodes (Figure 8b) to ensure sufficient contact between the triboelectric layers. As plotted in Figure 8c, the peak value of output power is  $50 \text{ W m}^{-3}$  at the load resistance of  $200 \text{ M}\Omega$  with 55 PTFE balls, which can light more than 200 LEDs. Moreover, it is successfully installed on an actual diesel engine to be a self-powered vibration sensor, which is demonstrated in Figure 8d. Given this design's high output and low-frequency adaptability, as shown in Figure 8e, Chang et al.<sup>[118]</sup> paralleled five layers of the HIS-TENG together to power ammonia leakage sensor for new energy ships by harvesting ship machinery's vibration energy triumphantly with

the power density of  $59.783 \text{ W m}^{-3}$ . This actual application exhibits the great potential of the TENG to be a sustainable and in situ power source for the wireless ammonia leakage sensor.

Other than installing different balls in relatively separate spaces,<sup>[119]</sup> many balls in one room is another way to further the power performance of the VEH. San et al.<sup>[117c]</sup> proposed a hybridized generator consisting of a cylindrical TENG (C-TENG) and a flexible thermal generator, which is shown in Figure 8f. C-TENG is composed of a transparent cylinder with two aluminum caps, which serve as electrodes and one of the tribo-materials, and PTFE beads, which serve as the triboelectrification inducing materials. In this study, PTFE beads with a 40% volume ratio (Figure 8f), which affects the output of C-TENG in aspects of contact area with the electrode and moving distance in the cylinder, are confirmed by investigating 10–90% volume ratios under vibration frequency of 5 Hz. After verifying the resonant frequency (15 Hz), durability, and the impact of different tilting angles under various vibrational forces, C-TENG could reach the highest power density of  $23.4 \text{ mW m}^{-3}$  at  $110 \text{ M}\Omega$ , which is shown in Figure 8g. To

accommodate more balls,<sup>[116]</sup> Pang et al. designed a matryoshka-inspired hierarchically structured TENG (HS-TENG) by nesting three-layer spherical shells,<sup>[50]</sup> as shown in Figure 8h. In Figure 8i, PTFE balls are filled into the gaps between the neighboring shells, and they will move back and forth on the surface of two Cu electrodes painted on shell under the actuation. Figure 8j shows the comparison of the output powers of the HS-TENG and a single ball TENG (SB-TENG) at 2 Hz. The output power of the HS-TENG is more than six times greater than that of the SB-TENG, reaching a maximum value of 544  $\mu\text{W}$ . In Figure 8k, the actual output performance is verified by powering an electronic watch after charging a capacitor. This kind of TENG with nest-assembling multiple shells can effectively harvest low-frequency mechanical vibration energy and easily achieve high output power density. Compared with traditional single-ball TENGs, these multi-ball designs improves space utilization and contact area in a limited volume, resulting in better energy harvesting performance.

### 4.3. Flat-Type VEH

According to the working principle of TENG, the larger contact area will bring more immediate power generation performance improvement. To achieve this, many flat-type VEHs with large

contact areas have been proposed. To begin with, as shown in Figure 9a, a contact-mode freestanding TENG (CF-TENG) consisting of FEP film, aluminum, and acrylic sheet connected by eight springs is employed by Wang et al. An acrylic plate with FEP films on both sides is designed as the vibration resonator. Energy harvesting is achieved by contacting and separating with two external aluminum electrode deposited acrylic plates under mechanical vibration,<sup>[51]</sup> which is illustrated in Figure 9b. To boost the output performance, the FEP film is treated by plasma etching to increase the surface charge density. Benefiting from the large surface area and high charge density, the maximum power density achieves 17  $\text{mW m}^{-2}$ . It could directly drive 60 LED under the vibration with an amplitude of 1.5 cm and frequency of 15 Hz. Furthermore, CF-TENG can convert the vibration energy to electricity during the operation of an actual wind blower, shown in Figure 9c. As depicted in Figure 9d, the maximum power density of CF-TENG reaches 17  $\text{mW m}^{-2}$  under the resonant frequency of 15 Hz and amplitude of 1.5 cm, which can directly light up 60 LEDs and show its potential to be an energy harvester.

Although some treatment method can enhance the charge density,<sup>[32,120]</sup> to boost the output power of the TENG, the single-layer TENG still face the challenge of low output power. To address the low output power of single-layer TENG and synchronize the output of different TENGs in multilayered TENG,

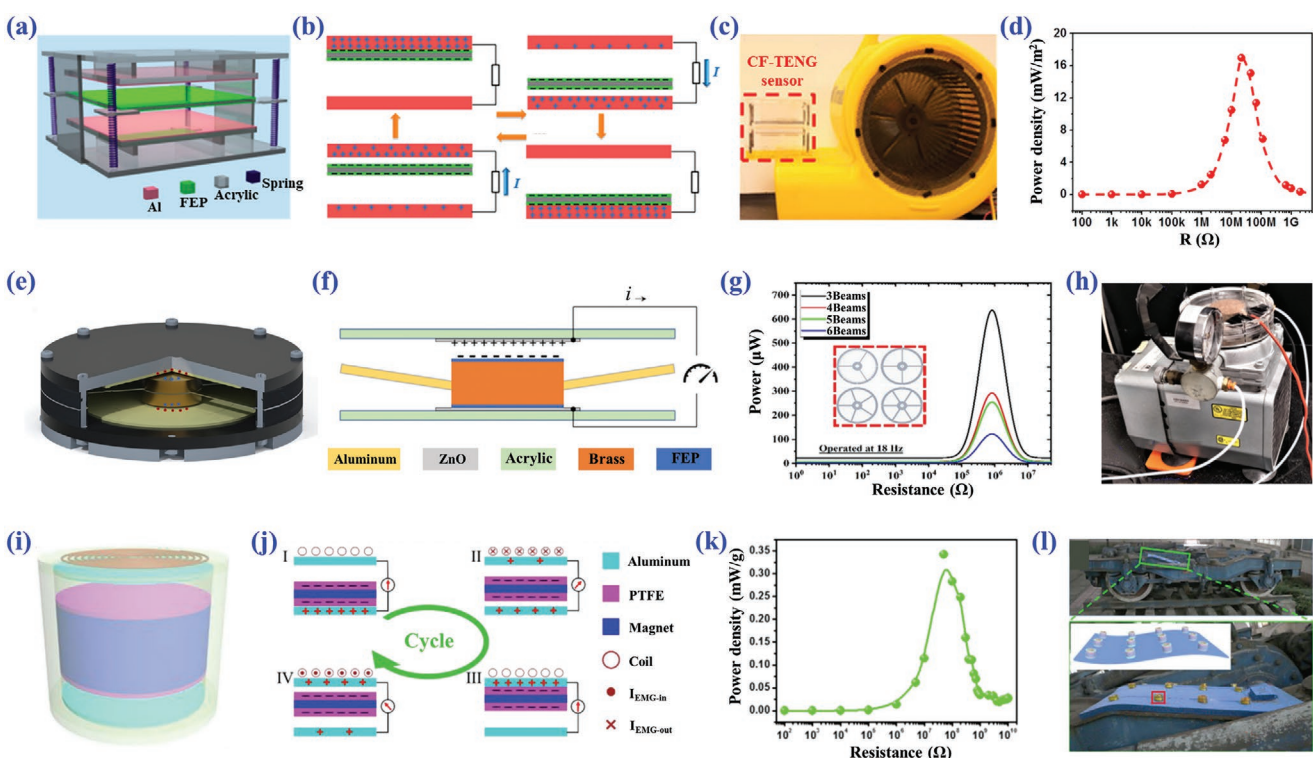


**Figure 9.** Flat-type VEH. a) Structure and b) working principle of the CF-TENG. c) Demonstration of the CF-TENG to monitor the vibration of a wind blower during its operation. d) Power density of CF-TENG under different resistances. Reproduced with permission.<sup>[51]</sup> Copyright 2014, American Chemical Society. e) Schematic structure of multi-cantilever-based vibration TENG. f) Step movements of brass block resulting in charge generations on active layers. g) Different maximum powers with three, four, five, and six beams in load matching experiment. h) Condition monitoring for a vacuum pump using the three-beam TENG. Reproduced with permission.<sup>[122]</sup> Copyright 2022, IOP Publishing. i) General illustration of MPNG. j) Working principle of MPNG including TENG and EMG. k) Calculated power density of the TENG on the different external loading resistances. l) Application of MPNG for energy harvesting from the train vibration. Reproduced with permission.<sup>[123]</sup> Copyright 2017, Elsevier.

a multilayered stacked TENG (3D-TENG) is reported by Yang et al.<sup>[75]</sup> The 3D-TENG is composed of some pinned and moveable fingers with all the fingers parallel to each other and eight identical springs used to bridge all the fingers. With the excitation by mechanical vibration, the moveable fingers go up and down with the assistance of springs. According to test results, the power density of 3D-TENG reaches  $104.6 \text{ W m}^{-2}$ , and it has effective response to the vibration frequency of 2–54 Hz. The design of the square plate and spring can also be seen in these works,<sup>[62,76]</sup> which is the typical structure of the earliest proposed TENG for vibration energy collecting. Even more, cubic-TENGs with an inside cube and outside cube are fabricated to accommodate multi-direction vibration.<sup>[121]</sup> The highest voltage of 500 V of the cubic-TENG is obtained in the SF<sub>6</sub> atmosphere, which achieves an increase of 67% compared to that in the air.<sup>[121a]</sup> Qiu et al. used the Fe balls inside the inner box to enhance the triboelectricity between the inner and the outer box.<sup>[121b]</sup>

Besides the square or similar flat type TENG, circular flat type TENG is another popular one. For instance, Prutvi et al. reported a multi-cantilever-based vibration TENG employing screen-printed ZnO film and FEP film as tribo-materials. The circular brass mass taking the role of a freestanding layer is fastened to some strip-type Al beams, which is depicted in Figure 9e.<sup>[122]</sup> In Figure 9f, ZnO film bonded to brass mass will contact upper and lower ZnO film successively under mechanical vibration, generating electricity with an effective reply to vibration frequency from 0 to 400 Hz. The maximum output power falls continuously as the number of beams increases. As shown in Figure 9g, the peak value of  $680 \mu\text{W}$  or  $1.38 \text{ W m}^{-2}$  is achieved by the three-beam architecture. This tunable design can adapt to different vibration conditions by adjusting the number of beams without major structural changes. As shown in Figure 9h, when the three-beam TENG is mounted on a vacuum pump, it is worth noting that it not only captures vibration frequency accurately, but also has the potential to be self-powering.

In addition to these flat-type VEH with the physical connection between the freestanding layer and the outer shell, Jin et al. integrated EMG and TENG to propose a maglev porous nanogenerator (MPEG) for the vibration of running trains,<sup>[123]</sup> as shown in Figure 9i. The middle magnet covered with porous PTFE, which acts as the freestanding layer of TENG and moves freely inside the shell without constraints by springs or beams, contacts the electrodes to be involved in electricity generation under the dual effects of the bottom magnet and vibration (Figure 9j). The porous structure provides a rough surface, leading to a larger effective contact area when the TENG is working. The instantaneous power density of the TENG has a maximum value of  $0.34 \text{ mW g}^{-1}$  at the resistance of  $50 \text{ M}\Omega$ , which is plotted in Figure 9k. And Figure 9l shows the energy harvesting from the train vibration in the train-running process by MPEG arrays. Given the characteristics of free-moving freestanding layer, many magnetically levitating flat-type VEHs based on TENG are invented. The nanogenerator proposed by He et al. can harvest vibration energy efficiently,<sup>[124]</sup> and the TENG delivers a peak output power of  $78.4 \mu\text{W}$  under 20 Hz. Kim et al. proposed a levitating oscillator-based TENG for harvesting energy from pendulum-like structures.<sup>[125]</sup> Using a

bridge rectifier, 21 and 61 commercial green LEDs were lit up by employing the 1 and 2 Hz inputs to the TENG, respectively. These works generally agreed that the levitated TENG is more sensitive than traditional mechanical suspension (like spring or cantilever). Thus, it prefers small energy collection and avoids mechanical fatigue or damage.

#### 4.4. Sliding Surface Type VEH

Sliding freestanding is another freestanding mode of TENG, which is also popular in VEH or vibration sensing. In this type, the freestanding layer alternately slides on two electrodes. The classic sliding block or sliding plate structure also appears in the TENG application. First, as shown in Figure 10a, Li et al.<sup>[52]</sup> reported a sliding block type TENG, which can convert the vibration of structures to electricity in AC and direct current (DC) mode with the name dual-mode TENG (AC/DC-TENG) to be a fully self-powered vibration monitoring system. The slider attached with a FEP film slides in a reciprocating manner between two friction electrodes under mechanical vibration, resulting in a back-and-forth flow of electrons between two friction electrodes. When a part of the slider moves off the edge of the electrode, air breakdown occurs because of the strong electric field under a tiny gap, resulting in a DC signal in the external circuit and driving the alarm light directly. AC/DC-TENG is applied to a bridge model, as displayed in Figure 10b. When the slider works under safe vibration, the mechanical energy will be converted into electrical energy by AC mode and stored in a capacitor. Then, if the slider slides out of the safe zone under abnormal vibration, the DC produced by the DC mode drives the red LED light in real-time. The energy produced by the AC mode, with a peak power of about  $50 \mu\text{W}$ , can provide the power for wirelessly transmitting the vibration signal. Furthermore, to accomplish multi-direction mechanical vibration harvesting, Chen et al. proposed a freestanding plate connected with four radial springs for scavenging low-frequency vibration energy from arbitrary in-plane directions with a peak power of  $85.7 \mu\text{W}$  and successfully applied to harvest brake energy of a bicycle wheel.<sup>[126]</sup> Xia et al. installed a honeycomb-like three-electrode structure on the inner surface of a spherical shell to convert mechanical vibration energy to electricity in full space.<sup>[127]</sup> The inner mass-spring-slider in Pang's work rubs against the multi-walls of the outer shell.<sup>[128]</sup> More stereoscopically, sliding freestanding TENGs with the sleeve-tube structure are proposed and fabricated.<sup>[53,129]</sup> And Wu adopted the sleeve-tube structure in drill string vibration environment successfully.<sup>[130]</sup>

To further improve energy conversion efficiency, electrodes with uniform spacing and complementary triboelectric layers are set in some works,<sup>[114a,130b,131]</sup> and a nonlinear oscillator-based TENG is also proposed based on the grating structure to boost the output performance of VEH.<sup>[132]</sup> Among them, considering the oneness of vibration direction, this sleeve-tube structure TENG was also combined with EMG to form a magnetic suspension energy harvester.<sup>[53,129b,c,133]</sup> The magnetic floating embedded TENG proposed by Seol et al.<sup>[53]</sup> is shown in Figure 10c. The floating oscillator, as the freestanding layer, is composed of a core magnetic rod and porous PDMS

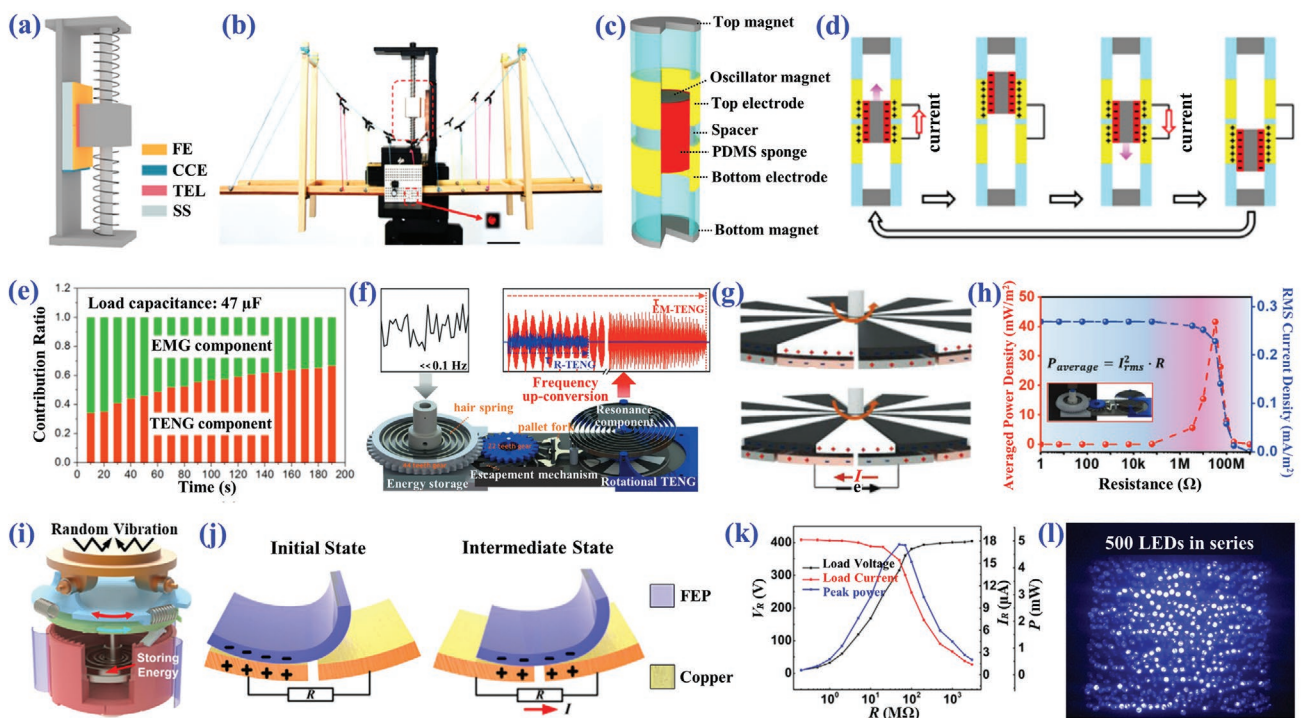


**Figure 10.** Sliding surface type VEH. a) The detailed structure of AC/DC-TENG. b) The photo of AC/DC-TENG on the bridge model. Reproduced with permission.<sup>[52]</sup> Copyright 2020, American Chemical Society. c) Schematics of the magnetic floating embedded TENG. d) Operating principle of the TENG component. e) Contribution ratio of the TENG and the EMG components with various charging times. Reproduced with permission.<sup>[53]</sup> Copyright 2016, Elsevier. f) Structure of EM-TENG. g) Schematic of the electricity generation principle of EM-TENG. h) Average power density and RMS current of EM-TENG with external load resistances. Reproduced with permission.<sup>[135a]</sup> Copyright 2020, Wiley-VCH. i) Schematics and j) working principle of the TSMR-TENG. k) Load-current, load-voltage, and peak power curves for the TSMR-TENG. l) 500 LEDs in series lit by the TSMR-TENG. Reproduced with permission.<sup>[136]</sup> Copyright 2020, Elsevier.

sponge surrounding the rod. In addition, the outer surface of the PDMS sponge is coated with PTFE, which serves two main roles. First, the porous sponge allows tight contact with the electrode for a larger contact area and triboelectric charge density.<sup>[65]</sup> Second, the PTFE layer reduces the frictional force at the sidewall, which results in smoother oscillation. As shown in Figure 10d, the freestanding oscillator floats in the tube by the bidirectional magnetic repulsion force and contacts with two aluminum electrodes up and down to generate current under the vibration excitation. The TENG component produces an output power of  $130 \text{ W kg}^{-1} \text{ m}^{-3}$  under the sinusoidal vibration with 7.5 Hz. Figure 10e is the contribution ratio of two components during charging, which proves that TENG subsequently provides a breakthrough at high consistency.

On the basis of above, some VEHs based on TENG for ultra-low-frequency energy harvesting are also invented.<sup>[134]</sup> In addition, disc structure TENGs<sup>[135]</sup> with comb-type sector electrodes in freestanding layer mode are also developed to harvest low-frequency mechanical vibration energy. Different from the 2D motion of the above VEHs, one of the key factors for disc TENGs to scavenge vibration energy is how to convert 2D mechanical vibration into sliding of the freestanding layers on the disc. Here, an escapement mechanism-based TENG (EM-TENG) was reported by Han et al. for harvesting extremely low-frequency irregular motions of less than 0.1 Hz.<sup>[135a]</sup> As shown in Figure 10f, the conversion mechanism inspired

by the mechanical watch consists of an escapement mechanism, an energy storage spring, and a torsional resonator. The energy storage spring captures irregular and low-frequency vibration energy. When the spring has been fully wound, the gear transfers energy to the spring-rotor part for generating regular and high-frequency rotational movement to drive the TENG. EM-TENG is operated in freestanding mode between the nylon film, PTFE film, and aluminum electrode. As shown in Figure 10g, when the rotator composed of nylon and PTFE moved, electrons in one electrode moved to another one to produce electric power. The average power density of EM-TENG is  $41 \text{ mW m}^{-2}$  under a low input frequency of 0.067 Hz, as shown in Figure 10h. More importantly, EM-TENG has great potential to be applied in irregular and extremely low frequency VEH existing in many structures.

Beyond the flat triboelectrification, Yang et al. presented a travel switch integrated mechanical regulation TENG (TSMR-TENG) equipped with circumferential flexible FEP films and copper electrodes.<sup>[136]</sup> The random vibration energy could be converted into electrical energy with a linear-rotational motion transformation mechanism and spiral spring, as shown in Figure 10i. The inertia wheel causes the flexible FEP film to slide against the copper electrodes to generate electric power,

which is illustrated in Figure 10j. As shown in Figure 10k,l, TSMR-TENG gets a peak output power of 5 mW at the resistance of 70 M $\Omega$  and can simultaneously light up 500 LEDs, which paves a way to widely applied to common random vibration environment, such as the vibration of bridges and passing over speed bumps by car. In brief, it is generally necessary for efficient low-frequency and irregular mechanical VEH to convert the conversion and storage mechanism into high-frequency and controllable mechanical energy as the input of TENG.

#### 4.5. Deformable Type VEH

Deformable materials have been broadly employed in various fields owing to their excellent adaptability.<sup>[137]</sup> Following these features, an increasing number of VEHs based on TENG adopt deformable materials as freestanding layers to achieve better shape adaptation to enhance triboelectric contact area to raise

output power.<sup>[138]</sup> Recently, by placing the flexible silicone rubber ring in the annular space of the drill pipe, a drill pipe-embedded annular type TENG (AT-TENG) was proposed by Du et al. to harvest arbitrary direction lateral vibration for the power supply of measurements while drilling system.<sup>[54]</sup> The structure of AT-TENG is shown in Figure 11a. The annular silicone rubber can fit closely better with the copper film attached to the inner surface of the outer tube. After contact, negative charges accumulate on the surface of the silicone rubber ring, and an equal amount of positive charge is induced on the copper film (Figure 11b). The moving status of the silicone rubber ring in AT-TENG is demonstrated by a high-speed camera, and its deformation increases the contacting area between silicone rubber and copper electrode with the increase of drill pipe vibration frequency or amplitude, thus enhancing the output performance. As shown in Figure 11c, the maximum output power density of the AT-TENG reaches 63.7 W m<sup>-3</sup> with a matching resistance of 400 M $\Omega$ . And AT-TENG shows appreciable output

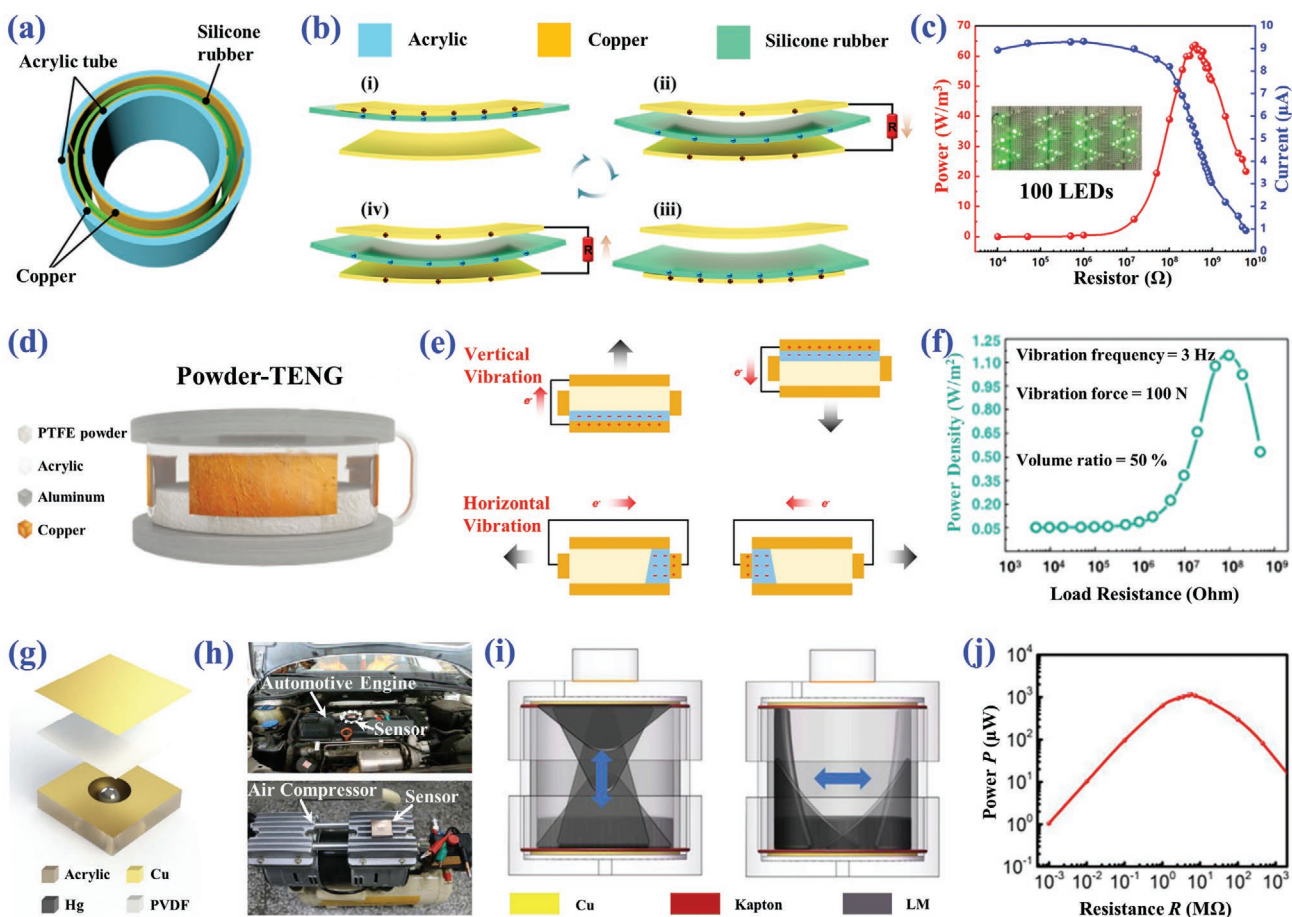


**Figure 11.** Deformable type VEH. a) Structure schematic and b) working principle of the AT-TENG. c) Measured output current and calculated output power-resistance profile for the AT-TENG. Reproduced with permission.<sup>[54]</sup> Copyright 2022, Wiley-VCH. d) Schematic illustration of the fabricated P-TENG. e) Detailed illustration of the electrical energy generation steps in the vertical vibration mode and horizontal vibration mode of the P-TENG. f) Load resistance dependency of the power density of the P-TENG with a volume ratio of 50% with vertical force of 100 N and a vibration frequency of 3 Hz. Reproduced with permission.<sup>[67c]</sup> Copyright 2016, American Chemical Society. g) Schematic diagram of the liquid metal TENG. h) Application scenario of the liquid metal TENG. Reproduced with permission.<sup>[56]</sup> Copyright 2017, American Chemical Society. i) Internal liquid flow of the liquid-metal-based freestanding TENG. j) Output power of the liquid-metal-based freestanding TENG at different load resistances. Reproduced under terms of the CC-BY license.<sup>[142a]</sup> Copyright 2021, Frontiers Media S.A.

performance when the lateral vibration direction changes in 360° direction. Meanwhile, the TENG enables lighting up more than 100 LEDs and powering a commercial temperature and humidity sensor successfully.

To pursue more extreme deformation, some works<sup>[55,67c,139]</sup> use triboelectric materials powder as freestanding layers. Kim et al. reported a P-TENG using PTFE power, as shown in Figure 11d.<sup>[67c]</sup> Two aluminum metal plates, which are nanostructured using a hydrothermal process by hot water, serve as the top and bottom electrodes and provide a larger contact surface area. Even more, four pieces of copper electrodes are attached to the outer side wall of the container in a configuration of two pairs facing each other. Due to fluid-like characteristics, the powder moves freely in 3D directions in the container, as depicted in Figure 11e. The working mode can be divided into two types: vertical mode and horizontal mode, which can harvest random mechanical vibrations in all directions. As displayed in Figure 11f, the output power is maximized with  $1.2 \text{ W m}^{-2}$  at a  $10^8 \Omega$  load with a vibration source of 3 Hz and is capable of powering 240 LEDs and charging a commercial battery. In addition, P-TENG also exhibits excellent durability against mechanical friction. Furthermore, because the powder has no specific shape, the structure can be designed rather freely, which leads to outstanding manufacturability regardless of size or shape of the container due to its fluid-like features, which provides a promising way to be durable and scalable VEHs for self-powered systems. Going extra miles, Lin et al. combined ceramic sheet with PTFE particles and silver particles mixed powder and designed layer-powder-layer structure TENGs to respond to ultra-high frequency vibration range of 3–133 kHz,<sup>[55]</sup> which can be utilized in track fracture detection, automobile engine monitoring, and geological exploration applications. Then a flexible piece structure is designed further to adapt to curved structures, such as pipelines, with the excellent reply to 3–170 kHz.<sup>[139b]</sup> It was especially pointed out that silver particles act as the electropositive triboelectric material to enhance the triboelectric effect in these works.<sup>[55,139b]</sup> Ferromagnetic particles are also applied in VEHs based on TENG to scavenge ambient mechanical energy.<sup>[139a,140]</sup>

Similarly, vibration energy harvesters introducing liquid medium has been the subject of active research recently, with advantages of shape adaptability, scalability, durability, and flexibility to subtle and irregular vibrations.<sup>[141]</sup> Therefore, liquid metal is a better choice for the liquid medium TENG and generally as a positive material.<sup>[56,142]</sup> Zhang et al. reported a liquid metal mercury droplet-based TENG,<sup>[56]</sup> as shown in Figure 11g. The structure and working principle are similar to those ball-TENGs',<sup>[34a,49,111]</sup> but the liquid metal mercury drop replaces the solid ball and is positively charged after contacting the triboelectric PVDF layers with nanofibers. And as shown in Figure 11h, they demonstrated that the liquid metal TENG fixed onto the air compressor and automotive engine to monitor the working state. In Figure 11i, Deng et al. used a large amount of liquid metal to obtain low-frequency and multi-directional vibration energy collection.<sup>[142a]</sup> When the TENG is excited by external vibration, the internal mercury collides between the surfaces of Kapton on both sides to generate electricity. Figure 11j demonstrated that the maximum output power of  $10^3 \mu\text{W}$  is obtained when the load resistance is  $8 \text{ M}\Omega$  and the constant frequency

is 10 Hz. To demonstrate the power generation capability more intuitively, 100 series-connected LEDs are lit up in the low-frequency environmental experiment successfully. The liquid-metal-based freestanding TENG can be placed in car suspension to harvest vibrational energy. Both shape adaptability and fluidity of this kind of deformable freestanding triboelectric layer increase the contact area and thus improve the output, which has a broad prospect in mechanical VEH for WSNs in the era of IoT.

In brief, one of the most significant core elements of the VEH based on freestanding mode TENG is the freestanding layer. In particular, different freestanding layer structures have an important influence on the vibration as well as the power generation characteristics of the VEH. According to the above description, VEHs based on the freestanding mode TENG can either have resonant characteristics such as the moving parts are restricted by elastic or magnetic force in flat-type or sliding surface type, or non-resonant characteristics such as the balls or powder moving freely in the VEH frame without restriction. Therefore, the freestanding mode VEH is both superior in adapting to efficient energy harvesting at resonant frequencies and achieving wide-frequency VEH by optimizing the freestanding layer. Meanwhile, the frame of the VEH can remain fixed and closed as the moving parts of the VEH based on freestanding layer mode TENG are inside the frame, which enables it to be widely adapted to the environment. Furthermore, it can be seen from the above different freestanding layers that the main means to enhance its output is to increase the triboelectric area. Excellent progress has been made in increasing the contact area to improve the output performance of the VEHs related to mechanical engineering. Besides, the charge density of the VEH based on freestanding mode TENG has also been enhanced by the surface modification of the electrodes and the freestanding layers. Meanwhile, the electrodes of most freestanding mode VEHs, such as some ball-type VEHs, and flat-type VEHs, are solid and fixed, which may lead to mismatching of the maximum contact area between tribo-materials, greater friction under uneven mechanical vibration, and performance deterioration under drastic mechanical vibration with high frequency if the freestanding layer is rigid and non-deformable as well. Sliding freestanding mode and deformable VEHs are emerged with optimal structure design to address this concern. Incredibly, although powder and liquid metal type VEH has outstanding adaptability to an extreme wide frequency range, the power (density) is relatively weak. Therefore, future research should concentrate on achieving the perfect combination of high performance and excellent response to wideband frequency mechanical vibration through novel structural design, deformable material selection, etc.

## 5. Conclusions and Perspectives

Vibration energy is omnipresent in the field of mechanical engineering, whereas the vast majority of it is underutilized. In the era of intelligence, it is of great significance to efficiently harvest the vibration energy related to mechanical engineering to be the sustainable and in situ power supply for tremendous

WSNs in the industrial and social fields. Over the past few decades, PVEHs and EMVEHs have been successfully applied in VEH. Since the TENG was invented, it has blazed a new way in substantial mechanical VEH and brought out a lot of fantastic achievements. In this paper, the recent advances in VEH based on TENG related to mechanical engineering have been summarized comprehensively and discussed systematically from the perspective of the most suitable working modes as C-S and freestanding mode.

A summary of structure characteristics and energy harvesting properties of some representative TENG-based VEHs with different working mode and structure is demonstrated in Table 1. The materials, output power (density), microstructure type, frequency range, applicable vibration direction, durability, application scenarios, and highlights are presented systematically for the first time. As shown in Table 1, these two different types of VEHs are featured with specific characteristics and are capable of performing respective advantages in different application scenarios. The VEHs based on C-S mode TENG can achieve high output at the resonant frequency and adapt to 2D direction VEH, while the VEHs based on freestanding mode TENG show advantages in multi-directional and broad bandwidth VEH. The most detailed summary of various VEHs based on TENG related to mechanical engineering is shown in Table S1, Supporting Information. It can provide a useful reference for researchers to design different VEHs properly to achieve optimal output performance with comprehensive consideration of the mechanical vibration characteristics and the application scenarios.

Through this study, it is anticipated that VEHs based on TENG will provide remarkable support for the alternative power supply of massive WSNs required in the era of intelligence. With the increasing demand for intelligence in the fields of mechanical engineering, embedded WSNs in machinery, vehicles, and structures are playing more and more significant roles in intelligent monitoring in the era of IoT. Therefore, it has become one of the developing orientations of the VEHs based on TENG to overcome the power supply problem and fully satisfy the self-powered demand of embedded WSNs by efficient mechanical VEH. Despite the fact that noticeable progress on VEH based on TENG is being accomplished, some challenges in energy conversion efficiency and practical application still need to be addressed to improve its future development (Figure 12).

### 5.1. Advanced Materials

The energy conversion of VEH based on TENG depends on the difference of triboelectric series of the tribo-materials to a great extent. So far, commercial polymer materials or compounds are generally applied to be the common tribo-materials. The inherent electron affinity of these existing materials hinders further promotion of energy conversion efficiency. Furthermore, common to many other fields, most polymer materials are difficult to be completely decomposed within a brief period under natural environment, which may cause a problem for final treatment of the tribo-materials. Therefore, it is urgent to create new tribo-materials, not only with superior electronegativity

and brilliant ability to charge capture and retention, but also with prominent environmental-friendly and recyclability.

### 5.2. Exquisite Configuration

Diversified latest designs have been developed to boost the energy conversion efficiency. However, VEH in higher degree broadband width and adaptability to irregular and multi-direction vibrations is required to be promoted nonetheless. To overcome this issue, the following two ways should be highly concerned. (1) Theoretical analysis: Disparate vibration features represent in different application fields related to mechanical engineering, and then issue in varying excitation mechanics. The configuration of the VEH based on TENG should be designed on the basis of comprehending the excitation mechanics in depth. (2) Manufacturing technique: Fabrication accuracy tends to affect the output performance of the TENG. Therefore, it is imperative to adopt or invent new manufacturing techniques to ensure configuration accuracy in light of in-depth theoretical research.

### 5.3. Charge Density Promotion

Boosting the charge density is another manner to increase the output of the VEH based on TENG to realize fully self-powered of the WSNs. Zou<sup>[144]</sup> and Xu et al.<sup>[145]</sup> have systematically summarized the physical and chemical modification ways for high-performance TENGs. However, the overwhelming majority of the existing methods fasten on the negative materials. Moreover, polarization and charge pump face the challenge of multifarious fabrication processes or complex structures of the VEH based on TENG. Therefore, epochal charge density lifting schemes are supposed to be created and applied to both positive and negative materials to promote the charge density of the VEH based on TENG.

### 5.4. Integration Capability

As we have mentioned, VEHs based on TENG related to mechanical engineering are principal to be the sustainable and in situ power supply for the WSNs. Nevertheless, TENGs with high voltage, low AC, and huge intrinsic impedance render severe difficulty in the integration between the VEH and the WSNs with low voltage and DC requirements.<sup>[146]</sup> As a result, PMC, which is used to accommodate the imbalance between supply and demand, becomes a promising way to integrate VEHs based on TENG and WSNs.<sup>[146]</sup> However, current PMCs are basically scheduled to specific TENG rather than universal for common use. Accordingly, the commonality and optimization of the PMCs are instant to be worked out. In addition, hybridization between VEH based on TENG and that based on other principles, such as PENG and EMG, ought to be given priority as well, which may achieve much more efficient mechanical VEH. Further, miniaturization and modularization of the VEHs and the integration system are always the development orientation of the VEHs based on TENG.

**Table 1.** A summary of structure characteristic and energy harvesting property of various TENG-based VEH.

| Mode         | Structure                        | Material           | Output                 | Microstructure                         | Frequency range               | Direction | Durability          | Application                                      | Highlight  | Ref.  |
|--------------|----------------------------------|--------------------|------------------------|--|-------------------------------|-----------|---------------------|--|--|-------|
| C-S          | Single spring/multilayer         | PTFE/Cu            | 2.5 mW (5 MΩ)          | Plasma-etching method                  | 2–25 Hz (resonance 15 Hz)     | 2D        | Over 500 000 cycles | Overhead transmission line                       | Six-layered helical structure/distributed manner                 | [64]  |
|              | Two plates/four corners-springs  | PVDF/wCF-PANI.Es   | 12.8 mW (1 MΩ)         | Nanopore/nanoflake                     | 5 Hz                          | 2D        | ≈11 000 cycles      | Harsh environment/medical application            | Chemical transform   | [78b] |
|              | Mass/four springs                | FEP/Cu             | 25 mW                  | /                                      | 6–20 Hz (optimal 18 Hz)       | 2D        | 36 000 cycles       | The IoTs/smart factory                           | Dual TENGs system/autonomous wireless frequency monitoring       | [40]  |
|              | Arch                             | PVDF/nylon         | 37.1 mW (9 MΩ)         | Nanowire                               | 5 Hz                          | 2D        | 36 000 cycles       | Powering DC motor/UVR detection device           | Nanostructure  | [41a] |
|              | Patch                            | PET/Al             | 6.5 μW cm⁻²            | /                                      | 10–100 Hz (resonance 30 Hz)   | 2D        | /                   | Coolant loop pipe in a nuclear power plant       | Vibration visualization sensor system/image processing method    | [41h] |
|              | Multilayer zigzag structure      | FEP/Al             | 19 mW (=0.8 MΩ)        | Plasma etching/electrochemical etching | 2–30 Hz (resonance 7 Hz)      | 2D        | /                   | Machine/riding bicycle                           | Elastic multiunit/power management circuit for DC                | [89]  |
|              | Trapezoidal cantilever structure | PET/Al             | 1.2 mW (10 MΩ)         | Plasma etching                         | 1–22 Hz (optimal 15 Hz)       | 2D        | 200 000 cycles      | Self-powered electronic system                   | Wide-range/integrated TENG array                                 | [44]  |
|              | Triple-cantilever beam/mass      | PDMS/Cu            | 252.3 mW m⁻² (0.25 MΩ) | Nanowire                               | 2.5–5 Hz (resonance 3.7 Hz)   | 2D        | 100 000 cycles      | Self-powered electronics                         | Surfacemodification/low-frequency                                | [96]  |
|              | Two cantilevers                  | FEP/Cu             | 4.31 mW (70 MΩ)        | /                                      | 3.5 Hz–50 Hz (optimal 4.1 Hz) | 2D        | 12 h                | Transmission line                                | Vibration attenuation/change resonant frequency                  | [105] |
|              | Cantilever-beam array            | PTFE/Al            | 30.95 mW               | Sanded                                 | 2–5 Hz (optimal 5 Hz)         | 2D        | 30 days             | Drill pipe                                       | Array-type/Measurement While Drilling                            | [45]  |
| Freestanding | Spherical shell/single ball      | silicone rubber/PS | 18 μW (200 MΩ)         | Inverted pyramid structure             | 1–3 Hz (optimal 3 Hz)         | Arbitrary | /                   | Ocean/large mechanical vibration equipment       | TENG-EMG/multilayer spherical shells/3D full-space               | [67b] |
|              | Spherical shell/single ball      | PTFE/Cu            | ≈0.011 μW (10 Ω)       | /                                      | 0.5–8 Hz (optimal 8 Hz)       | Arbitrary | 10 000 times        | Low-speed drilling                               | Downhole   | [111] |
|              | Two plates/multi-ball            | PTFE/Cu            | 50 W m⁻³ (200 MΩ)      | /                                      | 10–60 Hz (optimal over 35 Hz) | 2D        | 7 days              | Ship machinery                                   | Honeycomb structure/real ship test                               | [47]  |
|              | Two plates/multi-ball            | PTFE/Cu            | 59.783 W m⁻³ (11 MΩ)   | /                                      | 33.3 Hz                       | 2D        | 3 weeks             | Ammonia leakage monitoring device/ship machinery | Real ship application  | [118] |
|              | Plate–plate/cantilever-mass      | FEP/ZnO            | 680 μW                 | Screen-printed                         | 1–400 Hz (optimal 18 Hz)      | 2D        | /                   | Vacuum pump                                      | Tunable frequency response/detecting machinery fault             | [122] |
| Sliding      | Plate–plate                      | PTFE/Al            | 0.34 mW g⁻¹ (50 MΩ)    | Porous structure                       | 20 Hz                         | 2D        | /                   | High speed train                                 | TENG-EMG/self-powered wireless smart sensor/real-time monitoring | [123] |
|              | Spring/slider                    | FEP/Cu             | 22 mW (100 MΩ)         | /                                      | 10–50 Hz (optimal 20 Hz)      | 2D        | /                   | Industrial IoTs                                  | Nonlinear oscillator/boosting output                             | [132] |
|              | Rotating disk                    | PTFE/PU            | 15.68 mW               | /                                      | 0–50 Hz                       | 2D        | /                   | Train wheel                                      | Power management   | [143] |

**Table 1.** Continued.

| Mode                    | Structure          | Material  | Output    | Microstructure          | Frequency range | Direction                           | Durability   | Application                              | Highlight | Ref. |
|-------------------------|--------------------|---|-----------|-------------------------|-----------------|-------------------------------------|--|--|-----------|------|
| Sandwich/flexible strip | silicone rubber/Al | $94.95 \text{ W m}^{-3}$<br>( $250 \text{ M}\Omega$ ) | Sanded    | 5–90 Hz (optimal 90 Hz) | 2D              | 14 days                             | Metro/vehicle/<br>ship/bridge/<br>power plant/<br>building | Soft structure/lower<br>startup limit    | [138]     |      |
| Two plates/powder       | PTFE/Al/Cu         | $1.2 \text{ W m}^{-3}$<br>( $100 \text{ M}\Omega$ )   | Nanograss | 1–300 Hz                | 3D              | 1 week<br>( $7 \times 10^6$ cycles) | IoTs   | Fluid-like characteristic/all directions | [67c]     |      |
| Cylindrical tube        | Kapton/Hg          | $\approx 1 \text{ mW}$ ( $8 \text{ M}\Omega$ )        | /         | 0–18 Hz                 | 3D              | 3500 s                              | Car suspension/<br>ocean                                   | Liquid metal                             | [142a]    |      |

## 5.5. Energy Storage

With progress of electronic technology, the power consumption of the WSNs is lower and lower, so the vibration energy harvested by TENG may exceed the power consumption of WSNs, which may lead to energy surplus. It will be an immense waste if the residual energy is discarded. At present, the most common storage mode is to charge a capacitor, but electric leakage and capacity limitation impede the development. Henceforward, alternative energy storage mode needs to be highlighted on the agenda.

## 5.6. Durability and Stability

Abrasion in the working process of the VEHs based on TENG excited by the mechanical vibration is inevitable, and it is against the durability and stability of TENGs. Scholars have tried various ways to solve this problem, such as non-contact design, soft materials, buffer design, and lubrication. Furthermore, liquid or self-healing material may provide new

enlightenment for us to address this issue. In addition, working environment factors relevant to machinery, vehicles, and structures, including high/low temperature, high humidity, dust contamination, and electromagnetic influence, will be adverse to its durability and stability. Therefore, waterproofing and electromagnetic shielding encapsulation are necessities in the development path of VEHs based on TENG related to mechanical engineering. On top of the above, extremely high/low temperature such as the exhaust gas area of the diesel engine (higher than  $180^\circ\text{C}$ <sup>[147]</sup>) and polar region (lower than  $-50^\circ\text{C}$ ), have proposed challenges for its durability and stability, which should be paid close attention.

## 5.7. Large-Scale Production

VEHs based on TENG have been proven to be a breakthrough in mechanical VEH due to their unique superiority. The ultimate goal of VEHs based on TENG is practical application in mechanical VEH. Although some VEHs based on TENG verge on maturity to harvest mechanical vibration energy are



**Figure 12.** Challenges and perspectives of VEH based on TENG. Reproduced under terms of the CC-BY license.<sup>[142a]</sup> Copyright 2021, Frontiers Media S.A. Reproduced with permission.<sup>[135a]</sup> Copyright 2020, Wiley-VCH. Reproduced with permission.<sup>[91a]</sup> Copyright 2014, American Chemical Society. Reproduced with permission.<sup>[97]</sup> Copyright 2016, Springer Nature. Reproduced with permission.<sup>[40]</sup> Copyright 2022, Elsevier. Reproduced under terms of the CC-BY license.<sup>[78d]</sup> Copyright 2021, MDPI.

successively applied in natural working environments, it is still a long way to large-scale production. Not only technical aspects but also commercial aspects are requested to make more efforts.

The above challenges are also opportunities for researchers all over the world. Along with the further development of intelligence, we always keep the faith that VEHs based on TENG will play more and more crucial roles in mechanical VEH in the near future.

## Supporting Information

Supporting Information is available from the Wiley Online Library or from the author.

## Acknowledgements

T.D. and F.D. contributed equally to this work. This paper was funded by the National Natural Science Foundation of China (Grant Nos. 52101345 and 52101400), Scientific Research Fund of the Educational Department of Liaoning Province (Grant No. LJKZ055), Dalian Outstanding Young Scientific and Technological Talents Project (2021RJ11), and Fundamental Research Funds for the Central Universities (3132022211).

## Conflict of Interest

The authors declare no conflict of interest.

## Keywords

mechanical engineering, mechanical vibration, triboelectric nanogenerators, vibration energy harvesting

Received: January 13, 2023

Revised: February 4, 2023

Published online:

- [1] C. Zhang, Y. Lu, *J. Ind. Inf. Integr.* **2021**, *23*, 100224.
- [2] H. Qin, G. Cheng, Y. Zi, G. Gu, B. Zhang, W. Shang, F. Yang, J. Yang, Z. Du, Z. L. Wang, *Adv. Funct. Mater.* **2018**, *28*, 1805216.
- [3] Q. Y. Zhu, M. J. Guan, Y. Q. He, presented at *IEEE Int. Conf. on Information and Automation (ICIA)*, Shenyang, China, June and 2012.
- [4] W. Jie, F. Yao-Tian, *Phys. Procedia* **2012**, *24*, 961.
- [5] a) L. G. Xie, Y. Shi, Y. T. Hou, W. J. Lou, *IEEE Wireless Commun.* **2013**, *20*, 6; b) E. Sardini, M. Serpelloni, *IEEE Trans. Instrum. Meas.* **2011**, *60*, 1838; c) M. Jafari, K. Khan, L. Gauchia, *J. Energy Storage* **2018**, *20*, 67.
- [6] L. Zhang, M. H. Wong, *Environ. Int.* **2007**, *33*, 108.
- [7] N. Kannan, D. Vakeesan, *Renewable Sustainable Energy Rev.* **2016**, *62*, 1092.
- [8] G. M. J. Herbert, S. Iniyan, E. Sreevalsan, S. Rajapandian, *Renewable Sustainable Energy Rev.* **2007**, *11*, 1117.
- [9] A. F. D. O. Falcão, *Renewable Sustainable Energy Rev.* **2010**, *14*, 899.
- [10] L. Jian, H. Okada, T. Itoh, T. Harada, R. Maeda, *IEEE Sens. J.* **2014**, *14*, 2035.

- [11] a) F. U. Khan, *J. Renewable Energy* **2016**, *8*, 044702; b) M. Iqbal, M. M. Nauman, F. U. Khan, P. E. Abas, Q. Cheok, A. Iqbal, B. Aissa, *Int. J. Energy Res.* **2021**, *45*, 65.
- [12] C. Wei, X. Jing, *Renewable Sustainable Energy Rev.* **2017**, *74*, 1.
- [13] H. Yuan, H. Yu, X. Liu, H. Zhao, Y. Zhang, Z. Xi, Q. Zhang, L. Liu, Y. Lin, X. Pan, M. Xu, *Nanomaterials* **2021**, *11*, 3431.
- [14] M. He, W. Du, Y. Feng, S. Li, W. Wang, X. Zhang, A. Yu, L. Wan, J. Zhai, *Nano Energy* **2021**, *86*, 106058.
- [15] A. Nozariasbmarz, H. Collins, K. Dsouza, M. H. Polash, M. Hosseini, M. Hyland, J. Liu, A. Malhotra, F. M. Ortiz, F. Mohaddes, V. P. Ramesh, Y. Sargolzaeiaval, N. Snouwaert, M. C. Özturk, D. Vashaee, *Appl. Energy* **2020**, *258*, 114069.
- [16] J. Twiefel, H. Westermann, *J. Intell. Mater. Syst. Struct.* **2013**, *24*, 1291.
- [17] B. R. Ringeisen, E. Henderson, P. K. Wu, J. Pietron, R. Ray, B. Little, J. C. Biffinger, J. M. Jones-Meehan, *Environ. Sci. Technol.* **2006**, *40*, 2629.
- [18] J. Siang, M. H. Lim, M. S. Leong, *Int. J. Energy Res.* **2018**, *42*, 1866.
- [19] T. R. Lin, J. Pan, P. J. O'Shea, C. K. Mechefske, *Mar. Corros. Offshore Struct., Pap. Symp.* **2009**, *22*, 730.
- [20] S. Orhan, N. Akturk, V. Celik, *NDT E Int.* **2006**, *39*, 293.
- [21] K. J. Cheng, S. L. Lee, J. Y. Yang, presented at *2nd Int. Conf. on Civil Engineering, Architecture and Building Materials (CEABM 2012)*, Yantai, China, May and 2012.
- [22] J. Zhou, X. Zhao, K. Wang, Y. Chang, D. Xu, G. Wen, *Energy* **2021**, *228*, 120595.
- [23] G. Shi, J. Chen, Y. Peng, M. Shi, H. Xia, X. Wang, Y. Ye, Y. Xia, *Micromachines* **2020**, *11*, 80.
- [24] Y. Li, M. Misra, S. Gregori, presented at *57th IEEE Int. Midwest Symposium on Circuits and Systems (MWSCAS)*, College Station, TX, August and 2014.
- [25] W. Zhou, D. Du, Q. Cui, C. Lu, Y. Wang, Q. He, *Energies* **2022**, *15*, 947.
- [26] Y. Tan, Y. Dong, X. Wang, *J. Microelectromech. Syst.* **2017**, *26*, 1.
- [27] F. R. Fan, Z. Q. Tian, Z. L. Wang, *Nano Energy* **2012**, *1*, 328.
- [28] S. Niu, Z. L. Wang, *Nano Energy* **2015**, *14*, 161.
- [29] Z. L. Wang, T. Jiang, L. Xu, *Nano Energy* **2017**, *39*, 9.
- [30] Y. Zhou, M. Shen, X. Cui, Y. Shao, L. Li, Y. Zhang, *Nano Energy* **2021**, *84*, 105887.
- [31] a) C. Wu, A. C. Wang, W. Ding, H. Guo, Z. L. Wang, *Adv. Energy Mater.* **2019**, *9*, 1802906; b) W.-G. Kim, D.-W. Kim, I.-W. Tcho, J.-K. Kim, M.-S. Kim, Y.-K. Choi, *ACS Nano* **2021**, *15*, 258.
- [32] Y. Zou, J. Xu, K. Chen, J. Chen, *Adv. Mater. Technol.* **2021**, *6*, 2170016.
- [33] a) H. Y. Zou, Y. Zhang, L. T. Guo, P. H. Wang, X. He, G. Z. Dai, H. W. Zheng, C. Y. Chen, A. C. Wang, C. Xu, Z. L. Wang, *Nat. Commun.* **2019**, *10*, 9; b) R. Zhang, H. Olin, *EcoMat* **2020**, *2*, e12062.
- [34] a) T. Du, X. Zuo, F. Dong, S. Li, A. E. Mtui, Y. Zou, P. Zhang, J. Zhao, Y. Zhang, P. Sun, M. Xu, *Micromachines* **2021**, *12*, 218; b) C. Wu, H. Huang, S. Yang, G. Wen, *IEEE Sens. J.* **2020**, *20*, 13999; c) J. Y. Park, M. Salauddin, M. S. Rasel, J. *Micromech. Microeng.* **2019**, *29*, 053001.
- [35] a) J. Chen, Z. L. Wang, *Joule* **2017**, *1*, 480; b) L. Jin, B. Zhang, L. Zhang, W. Yang, *Nano Energy* **2019**, *66*, 104086; c) W. Kim, D. Bhatia, S. Jeong, D. Choi, *Nano Energy* **2019**, *56*, 307; d) J. Y. Shen, B. Li, Y. Yang, Z. Yang, X. Liu, K. C. Lim, J. Q. Chen, L. H. Ji, Z. H. Lin, J. Cheng, *Biosens. Bioelectron.* **2022**, *216*, 15; e) Z. L. Wang, *ACS Nano* **2013**, *7*, 9533; f) Z. L. Wang, J. Chen, L. Lin, *Energy Environ. Sci.* **2015**, *8*, 2250; g) X. Chen, Z. Ren, M. Han, J. Wan, H. Zhang, *Nano Energy* **2020**, *75*, 104980; h) H. Elahi, K. Munir, M. Eugeni, S. Atek, P. Gaudenzi, *Energies* **2020**, *13*, 5528; i) H. Ryu, H.-J. Yoon, S.-W. Kim, *Adv. Mater.* **2019**, *31*, 1802898;

- [36] A. A. Shabana, *Theory of Vibration: An Introduction*, Springer, New York 2018.
- [37] S. A. Graham, S. C. Chandrarathna, H. Patnam, P. Manchi, J. W. Lee, J. S. Yu, *Nano Energy* 2021, 80, 11.
- [38] X. Cao, Y. Xiong, J. Sun, X. Xie, Q. Sun, Z. L. Wang, *Nano-Micro Lett.* 2022, 15, 14.
- [39] M. Yuan, W. P. Yu, Y. W. Jiang, Z. J. Ding, Z. F. Zhang, X. Y. Zhang, Y. N. Xie, *Nano Energy* 2022, 103, 9.
- [40] X. H. Zhang, J. Q. Zhao, X. P. Fu, Y. Lin, Y. C. Qi, H. Zhou, C. Zhang, *Nano Energy* 2022, 9814, 107209.
- [41] a) Y. Zheng, L. Cheng, M. Yuan, Z. Wang, L. Zhang, Y. Qin, T. Jing, *Nanoscale* 2014, 6, 7842; b) L.-B. Huang, G. Bai, M.-C. Wong, Z. Yang, W. Xu, J. Hao, *Adv. Mater.* 2016, 28, 2744; c) S. A. Shankaregowda, C. B. Nanjegowda, X.-L. Cheng, M.-Y. Shi, Z.-F. Liu, H.-X. Zhang, *IEEE Trans. Nanotechnol.* 2016, 15, 435; d) J. Zhu, X. Hou, X. Niu, X. Guo, J. Zhang, J. He, T. Guo, X. Chou, C. Xue, W. Zhang, *Sens Actuators A Phys* 2017, 263, 317; e) H. Askari, Z. Saadatnia, A. Khajepour, M. B. Khamseee, J. Zu, *Adv. Eng. Mater.* 2017, 19, 1700318; f) C. Liu, L. Fang, H. Zou, Y. Wang, J. Chi, L. Che, X. Zhou, Z. Wang, T. Wang, L. Dong, G. Wang, Z. L. Wang, *Extreme Mech Lett* 2021, 42, 101021; g) H. Tao, J. Gibert, *Adv. Funct. Mater.* 2020, 30, 2001720; h) S.-J. Kim, M.-L. Seol, B.-Y. Chung, D.-S. Jang, J.-H. Kim, Y.-C. Choi, *Sensors* 2021, 21, 3976; i) H. Varghese, H. M. A. Hakkeem, K. Chauhan, E. Thouti, S. Pillai, A. Chandran, *Nano Energy* 2022, 98, 9.
- [42] Y. Du, J. Deng, P. Li, Y. Wen, *Nano Energy* 2020, 78, 105245.
- [43] Y. Chen, Y.-C. Wang, Y. Zhang, H. Zou, Z. Lin, G. Zhang, C. Zou, Z. L. Wang, *Adv. Energy Mater.* 2018, 8, 1802159.
- [44] Z. Ren, L. Wu, J. Zhang, Y. Wang, Y. Wang, Q. Li, F. Wang, X. Liang, R. Yang, *ACS Appl. Mater. Interfaces* 2022, 14, 5497.
- [45] Z. H. Lian, Q. Y. Wang, C. Q. Zhu, C. Zhao, Q. Zhao, Y. Wang, Z. Y. Hu, R. J. Xu, Y. K. Lin, T. Y. Chen, X. Y. Liu, X. Y. Xu, L. Liu, X. Xiao, M. Y. Xu, *Sensors* 2022, 22, 4287.
- [46] G. Tang, F. Cheng, X. Hu, B. Huang, B. Xu, Z. Li, X. Yan, D. Yuan, W. Wu, Q. Shi, *Electronics* 2019, 8, 1526.
- [47] X. Xiao, X. Zhang, S. Wang, H. Ouyang, P. Chen, L. Song, H. Yuan, Y. Ji, P. Wang, Z. Li, M. Xu, Z. L. Wang, *Adv. Energy Mater.* 2019, 9, 1902460.
- [48] H. Zhang, C. Yang, Y. Yu, Y. Zhou, L. Quan, S. Dong, J. Luo, *Nano Energy* 2020, 78, 105177.
- [49] L. F. Zhu, Z. C. Zhang, D. J. Kong, C. B. Liu, Z. G. Cao, W. Q. Chen, C. L. Zhang, *Nano Energy* 2022, 97, 107165.
- [50] Y. Pang, S. Chen, Y. Chu, Z. L. Wang, C. Cao, *Nano Energy* 2019, 66, 104131.
- [51] S. Wang, S. Niu, J. Yang, L. Lin, Z. L. Wang, *ACS Nano* 2014, 8, 12004.
- [52] S. Li, D. Liu, Z. Zhao, L. Zhou, X. Yin, X. Li, Y. Gao, C. Zhang, Q. Zhang, J. Wang, Z. L. Wang, *ACS Nano* 2020, 14, 2475.
- [53] M.-L. Seol, J.-W. Han, S.-J. Park, S.-B. Ron, Y.-K. Choi, *Nano Energy* 2016, 23, 50.
- [54] T. L. Du, F. Y. Dong, R. J. Xu, Y. J. Zou, H. Wang, X. J. Jiang, Z. Y. Xi, H. C. Yuan, Y. W. Zhang, P. T. Sun, M. Y. Xu, *Adv. Mater. Technol.* 2022, 7, 2200003.
- [55] Z. Lin, C. Sun, W. Liu, E. Fan, G. Zhang, X. Tan, Z. Shen, J. Qiu, J. Yang, *Nano Energy* 2021, 90, 106366.
- [56] B. Zhang, L. Zhang, W. Deng, L. Jin, F. Chun, H. Pan, B. Gu, H. Zhang, Z. Lv, W. Yang, Z. L. Wang, *ACS Nano* 2017, 11, 7440.
- [57] Z. L. Wang, *J. Phys. Commun.* 2022, 6, 085013.
- [58] Z. L. Wang, *Mater. Today* 2022, 52, 348.
- [59] C. Xu, Y. L. Zi, A. C. Wang, H. Y. Zou, Y. J. Dai, X. He, P. H. Wang, Y. C. Wang, P. Z. Feng, D. W. Li, Z. L. Wang, *Adv. Mater.* 2018, 30, 9.
- [60] Z. L. Wang, A. C. Wang, *Mater. Today* 2019, 30, 34.
- [61] H. Zhao, M. Shu, Z. Ai, Z. Lou, K. W. Sou, C. Lu, Y. Jin, Z. Wang, J. Wang, C. Wu, Y. Cao, X. Xu, W. Ding, *Adv. Energy Mater.* 2022, 12, 2201132.
- [62] G. Zhu, Z. H. Lin, Q. Jing, P. Bai, C. Pan, Y. Yang, Y. Zhou, Z. L. Wang, *Nano Lett.* 2013, 13, 847.
- [63] Y. Hu, J. Yang, Q. Jing, S. Niu, W. Wu, Z. L. Wang, *ACS Nano* 2013, 7, 10424.
- [64] H. Wu, J. Wang, Z. Wu, S. Kang, X. Wei, H. Wang, H. Luo, L. Yang, R. Liao, Z. L. Wang, *Adv. Energy Mater.* 2022, 12, 2103654.
- [65] K. Y. Lee, J. Chun, J.-H. Lee, K. N. Kim, N.-R. Kang, J.-Y. Kim, M. H. Kim, K.-S. Shin, M. K. Gupta, J. M. Baik, S.-W. Kim, *Adv. Mater.* 2014, 26, 5037.
- [66] Z. Cao, Z. Yuan, C. Han, J. Feng, B. Wang, Z. L. Wang, Z. Wu, *ACS Appl. Nano Mater.* 2022, 5, 11577.
- [67] a) J. Yang, J. Chen, Y. Yang, H. L. Zhang, W. Q. Yang, P. Bai, Y. J. Su, Z. L. Wang, *Adv. Energy Mater.* 2014, 4, 9; b) J. He, X. Fan, J. Mu, C. Wang, J. Qian, X. Li, X. Hou, W. Geng, X. Wang, X. Chou, *Energy* 2020, 194, 116871; c) D. Kim, Y. Oh, B.-W. Hwang, S.-B. Jeon, S.-J. Park, Y.-K. Choi, *ACS Nano* 2016, 10, 1017.
- [68] H. Liu, Y. Xia, T. Chen, Z. Yang, W. Liu, P. Wang, L. Sun, *IEEE Sens. J.* 2017, 17, 3853.
- [69] a) X. He, Q. Wen, Y. Sun, Z. Wen, *Nano Energy* 2017, 40, 300; b) A. Ibrahim, A. Ramini, S. Towfighian, *J. Sound Vib.* 2018, 416, 111; c) A. Ibrahim, A. Ramini, S. Towfighian, *Energy Rep.* 2020, 6, 2490; d) D. Nelson, A. Ibrahim, S. Towfighian, *J. Intell. Mater. Syst. Struct.* 2019, 30, 1745.
- [70] H. Deng, J. Ye, Y. Du, J. Zhang, M. Ma, X. Zhong, *Nano Energy* 2019, 65, 103973.
- [71] W. Guo, Y. Long, Z. Bai, X. Wang, H. Liu, Z. Guo, S. Tan, H. Guo, Y. Wang, Y. Miao, *Energy Convers. Manage.* 2022, 268, 115969.
- [72] L. Wang, T. He, Z. Zhang, L. Zhao, C. Lee, G. Luo, Q. Mao, P. Yang, Q. Lin, X. Li, R. Maeda, Z. Jiang, *Nano Energy* 2021, 80, 10555.
- [73] a) Z. Xia, P.-Y. Feng, X. Jing, H. Li, H.-Y. Mi, Y. Liu, *Micromachines* 2021, 12, 567; b) I. Mehamud, P. Marklund, M. Bjorling, Y. J. Shi, *Nano Energy* 2022, 98, 10.
- [74] Y. Qi, G. Liu, Y. Gao, T. Bu, X. Zhang, C. Xu, Y. Lin, C. Zhang, *ACS Appl. Mater. Interfaces* 2021, 13, 26084.
- [75] W. Yang, J. Chen, Q. Jing, J. Yang, X. Wen, Y. Su, G. Zhu, P. Bai, Z. L. Wang, *Adv. Funct. Mater.* 2014, 24, 4090.
- [76] J. Chen, G. Zhu, W. Yang, Q. Jing, P. Bai, Y. Yang, T.-C. Hou, Z. L. Wang, *Adv. Mater.* 2013, 25, 6094.
- [77] Y. Lin, Y. Qi, J. Wang, G. Liu, Z. Wang, J. Zhao, Y. Lv, Z. Zhang, N. Tian, M. Wang, Y. Chen, C. Zhang, *Sensors* 2022, 22, 3752.
- [78] a) D. Bhatia, W. Kim, S. Lee, S. W. Kim, D. Choi, *Nano Energy* 2017, 33, 515; b) R. K. Cheedarala, A. N. Parvez, K. K. Ahn, *Nano Energy* 2018, 53, 362; c) S. Kumar, R. Kumar, S. C. Jain, *Int. J. Green Energy*, <https://doi.org/10.1080/15435075.2022.2086001>; d) R. Li, H. Zhang, L. Wang, G. Liu, *Sensors* 2021, 21, 1514; e) M. Salauddin, R. M. Toyabur, P. Maharjan, M. S. Rasel, H. Cho, J. Y. Park, *Nano Energy* 2019, 66, 104122; f) H. H. Singh, D. Kumar, N. Khare, *Sustainable Energy Fuels* 2021, 5, 212; g) Z. Xu, D. Li, K. Wang, Y. Liu, J. Wang, Z. Qiu, C. Wu, J. Lin, T. Guo, F. Li, *Appl. Energy* 2022, 312, 118739; h) L. Zhang, L. Jin, B. Zhang, W. Deng, H. Pan, J. Tang, M. Zhu, W. Yang, *Nano Energy* 2015, 16, 516; i) X. Zhao, G. Wei, X. Li, Y. Qin, D. Xu, W. Tang, H. Yin, X. Wei, L. Jia, *Nano Energy* 2017, 34, 549; j) T. Quan, Y. Wu, Y. Yang, *Nano Res.* 2015, 8, 3272; k) A. A. Khan, A. Mahmud, S. Zhang, S. Islam, P. Voss, D. Ban, *Nano Energy* 2019, 62, 691; l) Y. Wang, Y. Wu, Q. Liu, X. Wang, J. Cao, G. Cheng, Z. Zhang, J. Ding, K. Li, *Energy* 2020, 212, 118462.
- [79] C. Wu, S. Yang, G. Wen, C. Fan, *Rev. Sci. Instrum.* 2021, 92, 055003.
- [80] D. Bhatia, H. J. Hwang, H. N. Dinh, S. Lee, C. Lee, Y. Nam, J.-G. Kim, D. Choi, *Sci. Rep.* 2019, 9, 8223.
- [81] M. Xu, P. Wang, Y.-C. Wang, S. L. Zhang, A. C. Wang, C. Zhang, Z. Wang, X. Pan, Z. L. Wang, *Adv. Energy Mater.* 2018, 8, 1702432.
- [82] a) K. Wang, J. Zhou, H. Ouyang, Y. Chang, D. Xu, *Mech. Syst. Signal Process.* 2021, 151, 107368; b) K. Wang, H. Ouyang, J. Zhou, Y. Chang, D. Xu, H. Zhao, *Meccanica* 2021, 56, 461.

- [83] D. Tan, J. Zhou, K. Wang, X. Zhao, Q. Wang, D. Xu, *Nano Energy* **2022**, *92*, 106746.
- [84] J. He, X. Fan, D. Zhao, M. Cui, B. Han, X. Hou, X. Chou, *Sci China Life Sci* **2021**, *65*.
- [85] X. Yang, J. Han, F. Wu, X. Rao, G. Zhou, C. Xu, P. Li, Q. Song, *RSC Adv.* **2017**, *7*, 50993.
- [86] X. Zheng, J. Su, X. Wei, T. Jiang, S. Gao, Z. L. Wang, *Adv. Mater.* **2016**, *28*, 5188.
- [87] Y. Song, X. Cheng, H. Chen, J. Huang, X. Chen, M. Han, Z. Su, B. Meng, Z. Song, H. Zhang, *J. Mater. Chem. A* **2016**, *4*, 14298.
- [88] X. Zhang, *Mater. Technol.* **2021**, *37*, 1611.
- [89] X. Wang, S. Niu, F. Yi, Y. Yin, C. Hao, K. Dai, Y. Zhang, Z. You, Z. L. Wang, *ACS Nano* **2017**, *11*, 1728.
- [90] a) W. Li, Y. Liu, S. Wang, W. Li, G. Liu, J. Zhao, X. Zhang, C. Zhang, *IEEE ASME Trans Mechatron* **2020**, *25*, 2188; b) H. Yang, M. Deng, Q. Zeng, X. Zhang, J. Hu, Q. Tang, H. Yang, C. Hu, Y. Xi, Z. L. Wang, *ACS Nano* **2020**, *14*, 3328.
- [91] a) X. Wen, W. Yang, Q. Jing, Z. L. Wang, *ACS Nano* **2014**, *8*, 7405; b) H. Li, R. Li, X. Fang, H. Jiang, X. Ding, B. Tang, G. Zhou, R. Zhou, Y. Tang, *Nano Energy* **2019**, *58*, 447; c) C. Garcia, I. Tredafirova, J. S. del Rio, *Nano Energy* **2019**, *56*, 443; d) G. Yang, Q. Shao, W. Li, L. Yang, L. Chen, M. Li, L. Ma, Y. Zhong, Z. Duan, *Macromol. Mater. Eng.* **2021**, *306*, 2000666; e) Q. Zhang, K. Barri, S. R. Kari, Z. L. Wang, A. H. Alavi, *Adv. Funct. Mater.* **2021**, *31*, 2105825.
- [92] a) S. Wang, L. Lin, Y. Xie, Q. Jing, S. Niu, Z. L. Wang, *Nano Lett.* **2013**, *13*, 2226; b) G. Zhu, J. Chen, Y. Liu, P. Bai, Y. S. Zhou, Q. Jing, C. Pan, Z. L. Wang, *Nano Lett.* **2013**, *13*, 2282.
- [93] a) S. Roundy, P. K. Wright, J. Rabaey, *Comput Commun* **2003**, *26*, 1131; b) S. Roundy, P. K. Wright, *Smart Mater. Struct.* **2004**, *13*, 1131; c) E. S. Leland, P. K. Wright, *Smart Mater. Struct.* **2006**, *15*, 1413.
- [94] a) H. S. Kim, J.-H. Kim, J. Kim, *Int. J. Precis. Eng. Manuf.* **2011**, *12*, 1129; b) A. M. Flynn, S. R. Sanders, *IEEE Trans Power Electron* **2002**, *17*, 8.
- [95] C. Y. Zhao, G. B. Hu, Y. W. Yang, *Mech Syst Signal Process* **2022**, *177*, 15.
- [96] W. Yang, J. Chen, G. Zhu, X. Wen, P. Bai, Y. Su, Y. Lin, Z. Wang, *Nano Res.* **2013**, *6*, 880.
- [97] T. Quan, Y. Yang, *Nano Res.* **2016**, *9*, 2226.
- [98] a) L. Dhakar, F. E. H. Tay, C. Lee, in *Int. Conf. on Experimental Mechanics* **2014**, Vol. 9302 (Eds: C. Quan, K. Qian, A. Asundi, F. S. Chau), SPIE, Bellingham, WA **2015**; b) L. Dhakar, F. E. H. Tay, C. Lee, *J. Microelectromech. Syst.* **2015**, *24*, 91.
- [99] C. Zhao, Y. Yang, D. Upadrashta, L. Zhao, *Energy* **2021**, *214*, 118885.
- [100] X. Du, S. Zhao, Y. Xing, N. Li, J. Wang, X. Zhang, R. Cao, Y. Liu, Z. Yuan, Y. Yin, Z. L. Wang, C. Li, *Adv. Mater. Technol.* **2018**, *3*, 1800019.
- [101] Y. Fu, H. Ouyang, R. B. Davis, *J Phys D Appl Phys* **2020**, *53*, 215501.
- [102] C. B. Williams, R. B. Yates, *Sens Actuators A Phys* **1996**, *52*, 8.
- [103] a) M. Ferrari, V. Ferrari, M. Guizzetti, D. Marioli, A. Taroni, *Sens. Actuators, A* **2008**, *142*, 329; b) I. Sari, T. Balkan, H. Kulah, *Sens. Actuators, A* **2008**, *145–146*, 405; c) H. Xue, Y. Hu, Q. M. Wang, *IEEE Trans Ultrason Ferroelectr Freq Control* **2008**, *55*, 2104.
- [104] M. Han, X. Zhang, W. Liu, X. Sun, X. Peng, H. Zhang, *Sci. China Technol. Sci.* **2013**, *56*, 1835.
- [105] S. T. Hu, Z. H. Yuan, R. N. Li, Z. Cao, H. L. Zhou, Z. Y. Wu, Z. L. Wang, *Nano Lett.* **2022**, *22*, 5584.
- [106] a) A. Hajati, S.-G. Kim, *Appl. Phys. Lett.* **2011**, *99*, 083105; b) L. Tang, Y. Yang, C. K. Soh, *J Intell Mater Syst Struct* **2010**, *21*, 1867; c) D. Zhu, M. J. Tudor, S. P. Beeby, *Meas. Sci. Technol.* **2010**, *21*, 022001;
- [107] a) R. H. Li, R. Y. Qiu, Y. H. Zhou, *Int J Non Linear Mech* **2018**, *105*, 268; b) A. Okninski, B. Radziszewski, *Int J Non Linear Mech* **2014**, *65*, 226.
- [108] R. Guo, K. Zhuo, X. Cui, W. Zhang, S. Sang, H. Zhang, *Energy Technol.* **2020**, *8*, 2000400.
- [109] Z. Wang, F. Zhang, N. Li, T. Yao, D. Lv, G. Cao, *Adv. Mater. Technol.* **2020**, *5*, 2000159.
- [110] H. Zhang, Y. Yang, Y. Su, J. Chen, K. Adams, S. Lee, C. Hu, Z. L. Wang, *Adv. Funct. Mater.* **2014**, *24*, 1401.
- [111] C. Wu, H. Huang, R. Li, C. Fan, *Sensors* **2020**, *20*, 1063.
- [112] a) C. Han, C. Zhang, W. Tang, X. Li, Z. L. Wang, *Nano Res.* **2014**, *8*, 722; b) G. Zhu, J. Chen, T. Zhang, Q. Jing, Z. L. Wang, *Nat. Commun.* **2014**, *5*, 3426.
- [113] J. Yang, Y. Sun, J. Zhang, B. Chen, Z. L. Wang, *Cell Rep Phys Sci* **2021**, *2*, 100666.
- [114] a) Q. Jing, G. Zhu, P. Bai, Y. Xie, J. Chen, R. P. S. Han, Z. L. Wang, *ACS Nano* **2014**, *8*, 3836; b) G. Zhu, Y. S. Zhou, P. Bai, X. S. Meng, Q. Jing, J. Chen, Z. L. Wang, *Adv. Mater.* **2014**, *26*, 3788.
- [115] a) X. H. Li, C. B. Han, T. Jiang, C. Zhang, Z. L. Wang, *Nanotechnology* **2016**, *27*, 085401; b) Q. Han, Z. Ding, Z. Qin, T. Wang, X. Xu, F. Chu, *Nano Energy* **2020**, *67*, 100717;
- [116] M. Xu, T. Zhao, C. Wang, S. L. Zhang, Z. Li, X. Pan, Z. L. Wang, *ACS Nano* **2019**, *13*, 1932.
- [117] a) C. B. Han, T. Jiang, C. Zhang, X. Li, C. Zhang, X. Cao, Z. L. Wang, *ACS Nano* **2015**, *9*, 12552; b) T. H. Choy, Y. O. Ying, F. Zhou, W. Xu, M. C. Wong, T. Ye, J. Hao, Y. Chai, *J. Mater. Chem. A* **2018**, *6*, 18518; c) S. T. San, J. Yun, D. Kim, *Nano Energy* **2022**, *97*, 107211;
- [118] J. Y. Chang, C. Q. Zhu, Z. M. Wang, Y. Wang, C. S. Li, Q. Hu, R. J. Xu, T. L. Du, M. Y. Xu, L. Feng, *Nano Energy* **2022**, *98*, 107271.
- [119] Y. Wang, T. Y. Chen, S. W. Sun, X. Y. Liu, Z. Y. Hu, Z. H. Lian, L. Liu, Q. F. Shi, H. Wang, J. C. Mi, T. M. Zhou, C. K. Lee, M. Y. Xu, *Nano Res.* **2022**, *15*, 3246.
- [120] H. S. Song, Y. J. Ko, D. Y. Kim, J. H. Jung, *Curr Appl Phys* **2016**, *16*, 1364.
- [121] a) S. Lv, B. Yu, T. Huang, H. Yu, H. Wang, Q. Zhang, M. Zhu, *Nano Energy* **2019**, *55*, 463; b) G. Qiu, W. Liu, M. Han, X. Cheng, B. Meng, A. S. Smitha, J. Zhao, H. Zhang, *Sci. China Technol. Sci.* **2015**, *58*, 842.
- [122] S. H. Prutvi, M. Korrapati, D. Gupta, *Meas. Sci. Technol.* **2022**, *33*, 075115.
- [123] L. Jin, W. Deng, Y. Su, Z. Xu, H. Meng, B. Wang, H. Zhang, B. Zhang, L. Zhang, X. Xiao, M. Zhu, W. Yang, *Nano Energy* **2017**, *38*, 185.
- [124] J. He, T. Wen, S. Qian, Z. Zhang, Z. Tian, J. Zhu, J. Mu, X. Hou, W. Geng, J. Cho, J. Han, X. Chou, C. Xue, *Nano Energy* **2018**, *43*, 326.
- [125] I. Kim, Y. Chae, S. Jo, D. Kim, *Nano Energy* **2020**, *72*, 104674.
- [126] X. Chen, H. Guo, H. Wu, H. Chen, Y. Song, Z. Su, H. Zhang, *Nano Energy* **2018**, *49*, 51.
- [127] X. Xia, G. Liu, H. Guo, Q. Leng, C. Hu, Y. Xi, *Nano Energy* **2015**, *15*, 766.
- [128] Y. K. Pang, X. H. Li, M. X. Chen, C. B. Han, C. Zhang, Z. L. Wang, *ACS Appl. Mater. Interfaces* **2015**, *7*, 19076.
- [129] a) H. Yu, X. He, W. Ding, Y. Hu, D. Yang, S. Lu, C. Wu, H. Zou, R. Liu, C. Lu, Z. L. Wang, *Adv. Energy Mater.* **2017**, *7*, 1700565; b) H. Askari, E. Asadi, Z. Saadatnia, A. Khajepour, M. B. Khamesee, J. Zu, *Nano Energy* **2017**, *32*, 105; c) X. Yang, C. Wang, S. K. Lai, *Eng. Struct.* **2020**, *221*, 110789.
- [130] a) W. Chuan, H. He, Y. Shuo, F. Chenxing, *Proc. Inst. Mech. Eng., Part C* **2021**, *235*, 6427; b) J. Liu, H. Huang, Q. Zhou, C. Wu, *IEEE Sens. J.* **2022**, *22*, 2250.
- [131] H. Deng, Y. Gao, R. Hu, S. Zhao, G. Han, X. Lian, M. Ma, X. Zhong, *Smart Mater. Struct.* **2021**, *30*, 115015.
- [132] D. Guan, G. Xu, X. Xia, J. Wang, Y. Zi, *ACS Appl. Mater. Interfaces* **2021**, *13*, 6331.
- [133] M.-L. Seol, J.-W. Han, S.-B. Jeon, M. Meyappan, Y.-K. Choi, *Sci. Rep.* **2015**, *5*, 16409.

- [134] a) C. Wang, S.-K. Lai, J.-M. Wang, J.-J. Feng, Y.-Q. Ni, *Appl. Energy* **2021**, *291*, 116825; b) X. Yang, S. K. Lai, C. Wang, J. M. Wang, H. Ding, *Energy* **2022**, *252*, 11.
- [135] a) K.-W. Han, J.-N. Kim, A. Rajabi-Abhari, V.-T. Bui, J.-S. Kim, D. Choi, I.-K. Oh, *Adv. Energy Mater.* **2021**, *11*, 2002929; b) K. Fan, D. Wei, Y. Zhang, P. Wang, K. Tao, R. Yang, *Nano Energy* **2021**, *90*, 106576; c) S. Gao, X. Zeng, G. Zhang, J. Zhang, Y. Chen, S. Feng, W. Lan, J. Zhou, Z. L. Wang, *Nano Energy* **2022**, *101*, 107530; d) Z. Qu, M. Huang, R. Dai, Y. An, C. Chen, G. Nie, X. Wang, Y. Zhang, W. Yin, *Nano Energy* **2021**, *87*, 106159; e) Z. Qu, R. Dai, L. Wu, Y. An, L. Chen, Y. Xie, Q. Wang, S. Jin, Z. Wang, W. Yin, *Nano Energy* **2020**, *76*, 105075.
- [136] W. Yang, Q. Gao, X. Xia, X. Zhang, X. Lu, S. Yang, T. Cheng, Z. L. Wang, *Extreme Mech Lett* **2020**, *37*, 100718.
- [137] a) S. Kwak, J. Kang, I. Nam, J. Yi, *Micromachines* **2020**, *11*, 347; b) E. Bury, S. Chun, A. S. Koh, *Adv. Electron. Mater.* **2021**, *7*, 2001006.
- [138] T. Du, B. Ge, A. E. Mtui, C. Zhao, F. Dong, Y. Zou, H. Wang, P. Sun, M. Xu, *Nanomaterials* **2022**, *12*, 1248.
- [139] a) V. Vivekananthan, A. Chandrasekhar, N. R. Alluri, Y. Purusothaman, G. Khandelwal, R. Pandey, S.-J. Kim, *Nano Energy* **2019**, *64*, 103926; b) Z. W. Lin, C. C. Sun, G. Q. Zhang, E. D. Fan, Z. H. Zhou, Z. Y. Shen, J. Yang, M. Y. Liu, Y. S. Xia, S. B. Si, J. Yang, *Nano Res.* **2022**, *15*, 7484.
- [140] D. Kim, I. K. Jin, Y.-K. Choi, *Nanoscale* **2018**, *10*, 12276.
- [141] a) M.-L. Seol, S.-B. Jeon, J.-W. Han, Y.-K. Choi, *Nano Energy* **2017**, *31*, 233; b) X. R. Yang, Y. Chen, Y. Zhang, W. R. Yang, *COMPEL* **2023**, *42*, 38; c) W. Wang, A. Yu, X. Liu, Y. Liu, Y. Zhang, Y. Zhu, Y. Lei, M. Jia, J. Zhai, Z. L. Wang, *Nano Energy* **2020**, *71*, 104605; d) B. Zhang, Z. Wu, Z. Lin, H. Guo, F. Chun, W. Yang, Z. L. Wang, *Mater. Today* **2021**, *43*, 37.
- [142] a) H. Deng, Z. Zhao, C. Jiao, J. Ye, S. Zhao, M. Ma, X. Zhong, *Front. Mater.* **2021**, *8*, 692273; b) K. Parida, G. Thangavel, G. Cai, X. Zhou, S. Park, J. Xiong, P. S. Lee, *Nat. Commun.* **2019**, *10*, 2158.
- [143] L. Jin, S. L. Zhang, S. Xu, H. Guo, W. Yang, Z. L. Wang, *Adv. Mater. Technol.* **2021**, *6*, 2000918.
- [144] Y. J. Zou, J. Xu, K. Chen, J. Chen, *Adv. Mater. Technol.* **2021**, *6*, 16.
- [145] J. Xu, Y. J. Zou, A. Nashalian, J. Chen, *Front Chem* **2020**, *8*, 23.
- [146] C. L. Fang, T. Tong, T. Z. Bu, Y. Z. Cao, S. H. Xu, Y. C. Qi, C. Zhang, *Adv. Intell. Syst.* **2020**, *2*, 17.
- [147] T. L. Du, F. Y. Dong, M. X. Zhu, Z. Y. Xi, F. M. Li, Y. J. Zou, P. T. Sun, M. Y. Xu, *J Mar Sci Eng* **2022**, *10*, 13.



**Taili Du** has been with Dalian Maritime University where he is currently an associate professor since 2010. He received his B.S. and M.S. from Dalian Maritime University in China in 2008 and 2010, and he is as a doctoral candidate in Marine Engineering College, Dalian Maritime University. His current research work focuses on vibration energy harvesting and self-powered vibration sensor based on triboelectric nanogenerator.



**Fangyang Dong** received his B.S. from Dalian Maritime University in China in 2019. Currently, he is as a postgraduate student in Marine Engineering College, Dalian Maritime University. His current research work focuses on triboelectric nanogenerator and artificial intelligence algorithm.



**Ziyue Xi** received his B.S. in 2020. Currently, he is as a postgraduate student in Marine Engineering College, Dalian Maritime University. His current research work focus on triboelectric nanogenerator and artificial intelligence algorithm.



**Meixian Zhu** received his B.S. in 2019. Currently, he is as a postgraduate student in Marine Engineering College, Dalian Maritime University. His current research work focus on triboelectric nanogenerator and artificial intelligence algorithm.



**Yongjiu Zou** is an assistant professor at College of Marine Engineering, Dalian Maritime University. He received his B.S. and M.S. in marine engineering both from Dalian Maritime University in 2012 and 2014, respectively. His research focuses on triboelectric nanogenerators for energy harvesting and self-powered sensors.



**Peiting Sun** received the Ph.D. degree in naval architecture and marine engineering from the Technical University Berlin, Germany, in 1993. From 1996 till now, he is a professor with marine engineering college, Dalian Maritime University. He is also a member of Naval Architecture and Ocean Engineering Discipline Appraisal Group of the State Council's Academic Degree Committee, an expert in the field of modern transportation technology in the National 863 Program, and a member of the Expert Committee of the Ministry of Transport. His research interests include green ship and intelligent ship operation and maintenance technologies.



**Minyi Xu** received his Ph.D. degree from Peking University in 2012. During 2016–2017, he joined Prof. Zhong Lin Wang' group at Georgia Institute of Technology. Now he is a professor in the Marine Engineering College, Dalian Maritime University. His current research is mainly focused on the areas of blue energy, self-powered systems, triboelectric nanogenerators, and its practical applications in smart ship and ocean.